

# Synthesis of a functional biomass lignin-based hydrogel with high swelling and adsorption of Acid Red 73

Shuxia Wei (✉ [wsx1120741959@163.com](mailto:wsx1120741959@163.com))

School of Chemistry and Environmental Engineering, Yangtze University, Jingzhou Hubei 434023, China

Wu Chen

School of Chemistry and Environmental Engineering, Yangtze University, Jingzhou Hubei 434023, China

Zhiming Tong

School of Chemistry and Environmental Engineering, Yangtze University, Jingzhou Hubei 434023, China

Nan Jiang

School of Chemistry and Environmental Engineering, Yangtze University, Jingzhou Hubei 434023, China

Mijia Zhu

School of Chemistry and Environmental Engineering, Yangtze University, Jingzhou Hubei 434023, China

---

## Research Article

**Keywords:** sodium lignosulfonate, hydrogel, AR 73, adsorption, dye wastewater

**Posted Date:** March 8th, 2021

**DOI:** <https://doi.org/10.21203/rs.3.rs-168152/v1>

**License:**  This work is licensed under a Creative Commons Attribution 4.0 International License.

[Read Full License](#)

---

# Synthesis of a functional biomass lignin-based hydrogel with high swelling and adsorption of Acid Red 73

Shuxia Wei , Wu Chen<sup>\*</sup>, Zhiming Tong, Nan Jiang, Mijia Zhu<sup>\*\*</sup>

(School of Chemistry and Environmental Engineering, Yangtze University, Jingzhou Hubei 434023, China)

<sup>\*</sup>Corresponding Author's E-mail: ccww91@126.com

**Abstract:** In this study, sodium lignosulfonate (LS) was used as raw material, acrylamide (AM) and acryloyloxyethyltrimethyl ammonium chloride (DAC) as monomers, and N,N'-methylenebisacrylamide (MBA) as cross-linking agent, the potassium persulfate (KPS)/tetramethylethyl enediamine (TEMED) as oxidation/reduction initiation system. Synthesis of a functional biomass terpolymer lignin-based hydrogel adsorbent (LAD) with excellent adsorption properties by free radical graft copolymerization. The structure and properties of the prepared LAD were characterized by FT-IR and SEM, and the relationship between structure and properties was studied. The effects of solution pH, adsorption time, hydrogel dosage, initial concentration of dye and temperature on the adsorption of AR 73 by LAD were investigated. LAD adsorbed AR 73 solution with initial concentration of 100mg/L for 2h to reach equilibrium, with equilibrium adsorption capacity and adsorption rate of 47.59mg/g and 95.18%, respectively. The prepared LAD hydrogel has good swelling and deswelling properties, the swelling ratio of water absorption for 2h was 25g/g, and the water loss rate of 120 min in ethanol solvent was 93.51%. The adsorption of AR 73 by LAD was consistent with the Langmuir isothermal adsorption model. It was single-molecule adsorption with a maximum adsorption capacity of 409.84mg/g. The adsorption was a process of spontaneous heat release and entropy reduction. The adsorption kinetics was in accordance with Pseudo-second-order kinetic equation, and the adsorption activation energy was 2.501 kJ/mol. In addition, the mechanism of adsorption is mainly electrostatic, and there are also comprehensive effects of physical, chemical adsorption and hydrogen bond. The LAD hydrogel adsorbent

has a significant adsorption effect on AR 73, and can be used as an efficient and recyclable biomass adsorbent for the treatment of anionic dye wastewater.

**Key words:** sodium lignosulfonate; hydrogel; AR 73; adsorption; dye wastewater

## Introduction

Lignin is the only aromatic polymer in nature, and its quantity is second only to cellulose (Rahul et al. 2017). The molecular structure of lignin contains many functional groups, such as carbonyl, methoxy, phenolic hydroxyl, alcohol hydroxyl, ether bond and conjugated double bond, and there are phenolic and non-phenolic aromatic rings. Its side chains and aromatic nuclei can be grafted and other chemical reactions, which can be used to prepare a variety of functional materials (Fan et al. 2004; Guo et al. 2008). However, so far, only a small part of lignin has been used to produce some chemicals or common polymer materials, and most of them have been burned directly (Feng and Chen 2011). Hydrogels are a kind of polymer with three-dimensional network structure that can swell in water and retain a large amount of water without dissolving (You et al. 2020). Hydrogel has the advantages of flexibility and biocompatibility, so it is widely used in the fields of industry, agriculture, environmental protection, medicine and biology (Lu et al. 2007; van de Manakker et al. 2010). However, the hydrogels prepared by traditional methods have low mechanical strength and poor stability, which greatly limits the application of hydrogels. In order to make full use of the advantages of abundant lignin, non-toxic, cheap, biodegradable and biocompatible, and at the same time improve the properties of hydrogel. Therefore, lignin-based hydrogels have become a new direction of high-value research and utilization of lignin. The use of lignin in the preparation of hydrogel can not only prepare products with certain properties, but also realize the resource utilization of lignin and reduce waste. At the same time, the introduction of lignin into the preparation of hydrogels are beneficial to enhance the strength of hydrogel (Lee and Yeh 2005).

Lignin-based hydrogels are mainly prepared in three ways (Yun et al. 2019): direct cross-linking method, grafting of lignin with hydrophilic monomers and

cross-linking agent at the same time, and lignin is introduced into the hydrogel in the form of interpenetrating or semi-interpenetrating. The molecular structure of lignin contains a large number of oxygen-containing functional groups, which are very important for the preparation of lignin-based hydrogels. In addition, these functional groups can generate electrostatic attraction between heavy metal ions or cationic dyes in wastewater (Chen et al. 2013), so as to achieve the removal of pollutants. Therefore, the hydrogel prepared from lignin can be used as an adsorbent in the field of wastewater treatment. At present, many researchers have used the above three methods to synthesize different lignin-based hydrogels and used them to adsorb heavy metal ions or dye wastewater, and achieved varying degrees of success (Peñaranda A and Sabino 2010; Wang et al. 2020; Xu et al. 2015; Yu et al. 2016). The results show that the adsorbed lignin-based hydrogels can be easily separated from the liquid phase, which can reduce the follow up separation work. However, at present, most reports use toxic and harmful organic solvents such as epichlorohydrin (Raschip et al. 2011) and dimethyl sulfoxide (El - Zawawy 2005; Feng 2012) to prepare lignin-based hydrogels. The use of a large number of organic solvents not only causes difficulties in wastewater treatment, but also reduces the environmental friendliness of lignin-based hydrogels. In addition, lignin-based hydrogels have some disadvantages such as low content of surface active groups and poor adsorption effect when they are used as adsorbents, so it is necessary to further increase the content of surface active groups of adsorbents (Zhang 2018b). Therefore, it is of great significance to find a relatively green solvent to replace the above toxic and harmful organic solvents to prepare biomass lignin-based hydrogels with high adsorption properties.

Based on the above research background, this study using lignin derivative lignosulfonate sodium(LS) as raw material, acrylamide (AM) and acryloyloxyethyltrimethyl ammonium chloride (DAC) as monomers, and N,N'-methylenebisacrylamide (MBA) as cross-linking agent, the potassium persulfate (KPS)/tetramethyl ethylenediamine (TEMED) as oxidation/reduction initiator system, through the free radical graft copolymerization to synthesize a functional biomass with excellent adsorption properties of terpolymer lignin-based hydrogel adsorbent(L

S-g-P (AM-co-DAC), LAD). The method has the advantages of simple process, easy operation, mild reaction conditions and effectively avoiding the use of toxic and harmful organic solvents or strong bases and strong acids, and is a green and environmentally friendly preparation method. DAC is a kind of multi-group cationic monomer, and the quaternary ammonium group ( $-\text{CH}_2-\text{N}^+(\text{CH}_3)_3$ ) in the molecule makes it strong cationic and hydrophilic, so it is the most widely used cationic monomer at present (Chen and Zhang 2019; Lee et al. 2012). It is precisely because of these characteristics that DAC is gradually used to prepare hydrogels and to treat anionic dye wastewater. The structure and properties of the prepared LAD were characterized by FT-IR and SEM. In this study, the adsorption properties of lignin-based hydrogels were investigated by taking the refractory azo dye Acid red 73 (AR 73) simulated wastewater as the research object. The adsorption kinetics, adsorption isotherm and adsorption thermodynamics of LAD were studied, and the adsorption mechanism was discussed. It provides a theoretical and scientific basis for the application of industrial lignin and hydrogel as adsorption materials in dye wastewater treatment, and provides a reference for the high-value utilization and popularization of biomass resources.

## Experimental section

### Materials and instruments

#### Materials

Sodium Lignosulfonate (LS), N, N'-methylene-bisacrylamide (MBA) were purchased from Tianjin Guangfu Fine Chemical Research Institute, acrylamide (AM) was obtained from Kemiou Chemical Reagent Co., Ltd., Tianjin(China). Potassium persulphate (KPS) was purchased from Beilian Fine Chemicals Development Co., Ltd., Tianjin(China). N,N,N',N'-Tetramethylethylenediamine(TEMED) and Acryloyloxyethyltrimethyl Ammonium Chloride (DAC) were brought from Yuanye Biological Technology Co., Ltd., Shanghai (China). Acid Red73 (AR 73) was provided by West Asia Chemical Industry Co.,Ltd., Shandong (Chi

na). All of the above chemicals were analytical grade. In this study, All the experimental water were deionized water.

### **Instruments**

ISO-9001 electronic analytical balance, HH-4 thermostatic water bath, Electric blast drying box and PHS-3 pH Meter were produced by Sartorius Scientific Instruments Co., Ltd (Beijing)., Guohua Electric Co., Ltd., Shanghai Yiheng Scientific Instrument Co., Ltd., Shanghai Electronic Scientific Instrument Co., Ltd. respectively. SHZ-82A Water-bathing Constant Temperature Vibrator, and SP-2100 visible light spectrophotometer were manufactured by Shanghai Spectral Instrument Co., Ltd. IR400 infrared spectrometer and JSM-6610lv Scanning Electron Microscope were produced by Shimadzu Corporation.

### **Preparation of LAD**

The preparation of lignin-based hydrogel adsorbent (LAD) was described as follows. First, LS (0.4g), AM (1.4g) and MBA (0.036g) were weighed accurately and dissolved in a beaker with a small amount of deionized water to obtain the solution A. Taking KPS (0.22g) was dissolved in another beaker with a small amount of deionized water to get the solution B. After preheating the two beakers in a constant temperature water bath for 10-30 minutes, and mixing the solution A and B of the two beakers and shake well. After then, TEMED (70  $\mu$ l) and DAC (0.7g) were added to the reaction system, which were quickly shaken and polymerized in a thermostatic water bath at 40°C. After continuous reaction for a period of time, LAD was obtained. Finally, the hydrogel was cut into small pieces and soaked in a large amount of distilled water for 3 days. The water was changed twice a day to remove unreacted substances from the hydrogel. The process of synthesis of LAD was shown in Fig. 1.

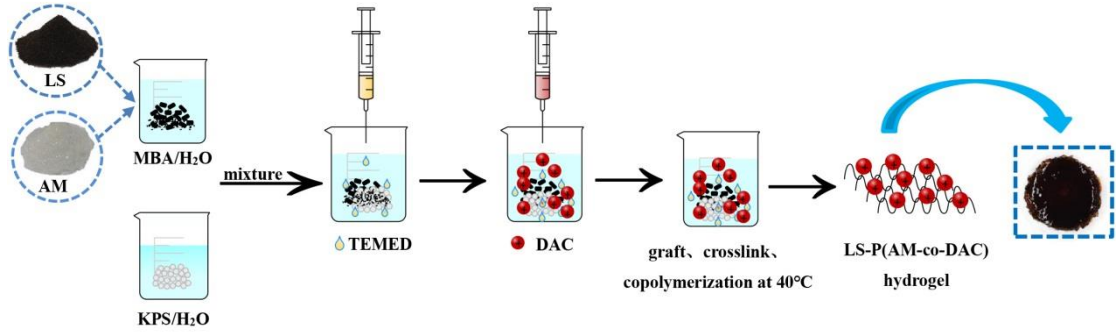


**Fig. 1** Schematic of the synthesis of LAD hydrogel

## Characterization of LAD

The inner structural interactions of LAD was measured by the Fourier transform infrared spectroscopy (FT-IR, Shimadzu Corporation, Japan) operating in the range of  $4000\sim 400\text{ cm}^{-1}$  and the resolution of  $4\text{ cm}^{-1}$ . SEM was used to analyze the surface morphology of the freeze-dried hydrogel with the JSM-6610lv Scanning Electron Microscope.

## Study on the performance of LAD

### Study on swelling and deswelling properties

The swelling and deswelling properties of LAD were determined by mass method. At room temperature, accurately weigh 0.10g dried hydrogel, put it into deionized water, take it out with tweezers at regular intervals, then wipe off the water on the hydrogel surface with filter paper, weigh it, and calculate its swelling ratio (SR) according to Formula (1). For the deswelling of LAD, the swelling equilibrium hydrogel was added to the ethanol solution, weighed according to the same method, and the deswelling rate (DR) was calculated according to Formula (2).

$$SR = \frac{m_t - m_o}{m_o} \quad (1)$$

$$DR = \left( \frac{m_t - m_o}{m_e} \right) \times 100\% \quad (2)$$

Where  $m_o$  is the mass of dry hydrogel, g;  $m_t$  is the mass of hydrogel at time t, g;  $m_e$  is the mass of hydrogel at swelling equilibrium, g.

### Study on adsorption performance

The effects of solution pH, adsorption time, adsorbent dosage, initial concentration of dye and temperature on the adsorption effect of LAD on AR 73 were investigated by single factor experiment of static adsorption.

First, accurately weigh a certain quality of dried hydrogel, put it in deionized water to make its swelling equilibrium at room temperature. After then, put it in a 150mL conical flask with stopper, added a certain concentration of 50mL AR 73 solution and adjusted pH. Finally, put the conical flask on a Water-bathing Constant Temperature Vibrator at a certain temperature, and carry out the oscillatory adsorption experiment with 150r/min. After a certain time of adsorption, the absorbance (A) of the supernatant was measured with a visible spectrophotometer at 509nm, and the residual concentration after adsorption was calculated by the standard curve. According to the concentration of the dye before and after adsorption, the adsorption amount  $Q_t$  (mg/g) and removal rate  $R$  (%) of the hydrogel to AR 73 are calculated. The adsorption capacity and removal rate can be calculated by the following formulas (3) and (4):

$$Q_t = \frac{(C_o - C_e) \times V}{m} \quad (3)$$

$$R = \frac{C_o - C_e}{C_o} \times 100\% \quad (4)$$

Where  $V$  is the volume of dye solution, mL;  $m$  is the mass of dry hydrogel, g;  $C_o$  and  $C_e$  represent the initial concentration and adsorption equilibrium concentration of the dye, mg/L, respectively.

### Regeneration of LAD

Under the adsorption conditions selected in the previous stage, the hydrogel after AR 73 equilibrium was adsorbed for the first time and put into 100 mL of nitric acid solution. After desorption at room temperature for 2h, the hydrogel was removed, washed with deionized water and dried in a drying oven. The regenerated hydrogel samples were re-adsorbed according to 1.4.2 experimental method, and 10

consecutive adsorption and desorption experiments were carried out to explore the regeneration performance of LAD.

## Results and discussions

### Analysis of LAD synthesis mechanism

The synthesis mechanism of LAD is shown in Fig. 2. As shown in Fig 2, under the excitation of TEMED as reducing agent, initiator KPS first produced initial free radical  $2SO_4^{\bullet-}$ , which reacted with AM monomer to form acrylamide free radical monomer. Under the action of cross-linking agent, the free radical monomer and cross-linking agent were grafted and copolymerized to form a polymer with three-dimensional network structure (Wang et al. 2020). In addition, the free radical reacted with LS and DAC near the reaction site, causing the chain to initiate and then become the free radical donor of the adjacent molecule, extending its spatial structure. In the process of polymerization, free radical monomers were grafted with LS and DAC, chain growth reaction was carried out to form chain polymers. Under the action of the cross-linking agent, the polymers were cross-linked and polymerized to form a terpolymer, which was the LAD hydrogel adsorbent.

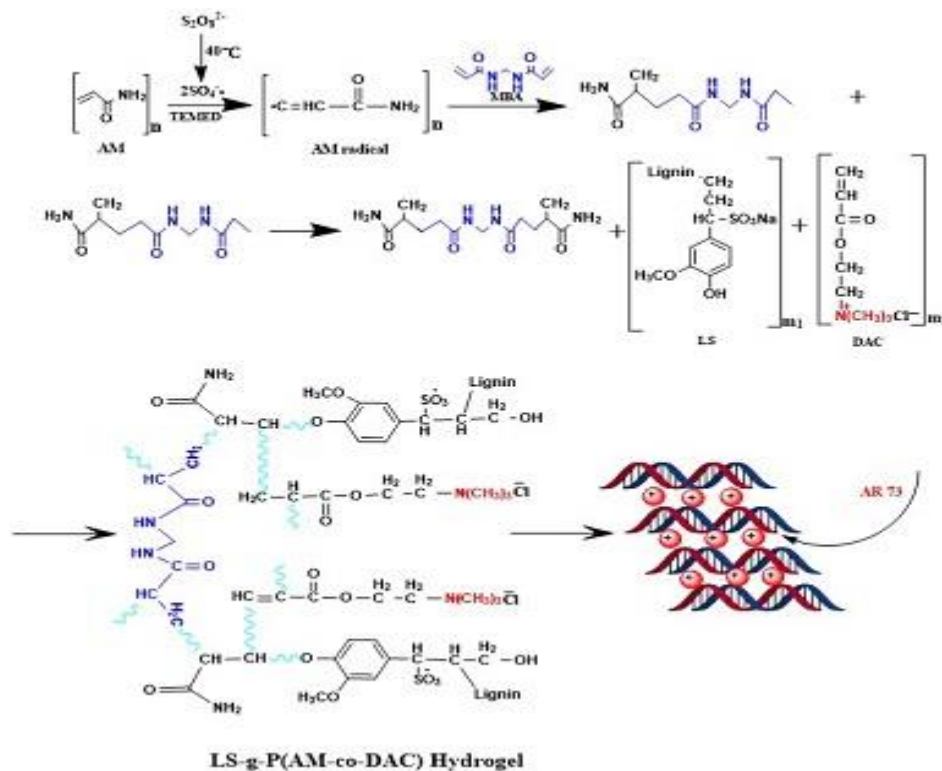
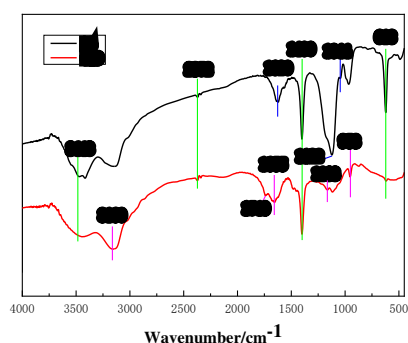


Fig. 2 The synthesis mechanism of LAD hydrogel

## Analysis of LAD characterization

### FT-IR analysis

The infrared spectrum analysis of LS, LAD and LAD-AR 73 as shown in Fig. 3 and 4. As can be seen from Fig. 3, there is a broad peak located at  $3443\text{cm}^{-1}$ , attributing to the O-H stretching vibration of phenol or polyol in the molecular structure of LS. The absorption peak at  $1620\text{ cm}^{-1}$  and  $1516\text{ cm}^{-1}$  were the stretched vibration of C=C on the aromatic ring skeleton, which are the characteristic absorption peak of lignin. A characteristic peak around  $1122\text{ cm}^{-1}$  ascribes to the asymmetric stretching vibration absorption peak of C-O-C on the aromatic ring, and the peak appears at  $1044\text{ cm}^{-1}$  is attributable to asymmetric stretching vibration of the S=O in sulfonic acid groups. The absorption peak at  $618\text{ cm}^{-1}$  is attributed to the C-S stretching vibration (Shao et al. 2009). Comparing the infrared spectrum of LS, there are new characteristic absorption peaks at  $3160\text{cm}^{-1}$  and  $1655\text{ cm}^{-1}$  in LAD, which are derived from the symmetric stretching vibration of N-H and the -C=O stretching vibration of -CONH<sub>2</sub>. This showed that AM was successfully grafted on the LS chain. In addition, the stretching absorption peak of ester groups (at  $1740\text{ cm}^{-1}$ ), the contraction and bending vibration of methyl (-CH<sub>3</sub>) in (-CH<sub>2</sub>-N<sup>+</sup>(CH<sub>3</sub>)<sub>3</sub>) ( $1163\text{ cm}^{-1}$ ) and the characteristic absorption peak of (-CH<sub>2</sub>-N<sup>+</sup>(CH<sub>3</sub>)<sub>3</sub>) ( $953\text{ cm}^{-1}$ ) appeared in the LAD spectrum. This also confirmed that DAC was successfully grafted onto LS. Comparing the two maps, LAD roughly retains the basic structure of LS, and contains the functional groups of AM and DAC.



**Fig. 3** FT-IR spectra of LS and LAD hydrogel adsorbent

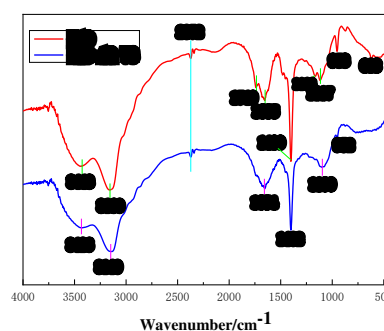


**Fig. 4** FT-IR spectra of LAD hydrogel adsorbent before and after dye adsorption

It can be seen from Figure 4 that compared with the infrared spectrum of LAD, the infrared spectrum of LAD after adsorption of AR 73 has changed. After adsorption of AR73, the O-H stretching vibration absorption peak ( $3443\text{ cm}^{-1}$ ) and the C-O-C stretching peak ( $1117\text{ cm}^{-1}$ ) of the phenolic alcohol on the aromatic ring have some blue shifts, indicated that there were hydrogen bond interaction between the part-OH and AR 73 molecules. The N-H stretch peak ( $3160\text{ cm}^{-1}$ ) also has a blue shift and the peak shape is slightly wider. The -CH- stretching vibration peak ( $1402\text{ cm}^{-1}$ ) on the aromatic ring skeleton has a slight red shift, and the intensity is also weakened. Besides, the ester absorption peak ( $1740\text{ cm}^{-1}$ ) in DAC and the stretching peak of C-S ( $618\text{ cm}^{-1}$ ) on the LS skeleton disappeared. These changes indicated that there were interaction and chemisorption between LAD and AR 73.

### SEM analysis

The SEM image of LAD hydrogel after freeze-drying under different magnifications were shown in Fig. 5. It can be seen from the Fig. 5 that the surface of LAD hydrogel showed a three-dimensional network structure (Ai et al. 2020), with regular distribution of honeycomb pores with voids size ranging from a few microns to dozens of microns. These pores provide channels for water transport. In the case of ordinary vacuum drying the pore structure of LAD hydrogel will be collapsed and destroyed due to the loss of water during the drying process, and the real reticular structure of hydrogel can not be well observed. However, the three-dimensional reticular pore structure of the hydrogel can be well maintained by freeze-drying, and the hydrophilic groups in the hydrogel absorb a large amount of water inside the hydrogel. These water molecules act as pore-forming agents. the honeycomb pore structure is formed by sublimation and escape of freeze-dried water molecules (Sun et al. 2016). For the porous structure of hydrogel, the unidirectional porous structure on the surface is beneficial to promote the diffusion of AR 73, thereby effectively improving the adsorption effect.

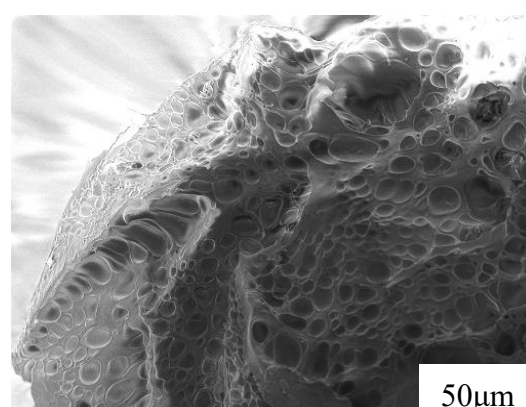
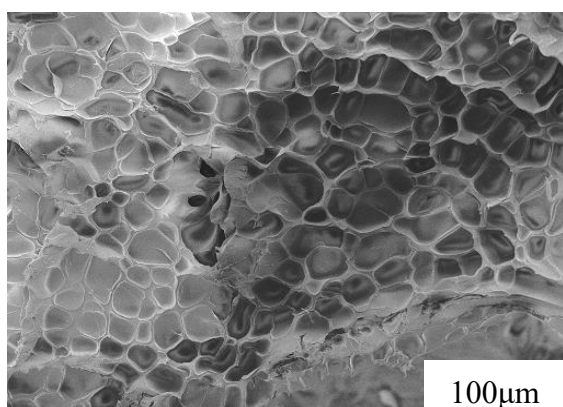


**Fig. 5** SEM images of LAD hydrogels at different magnification

## **Swelling and deswelling analysis of LAD**

Swelling and deswelling are two aspects of the volume phase transition of environmentally sensitive hydrogels, and they are important characteristics of hydrogel intelligence. The swelling or shrinkage process of the hydrogels are mainly reflected in the interaction between the hydrophilic groups, the hydrophobic groups and the solvent in the hydrogel. Since LAD hydrogels contain hydrophilic groups such as sulfonic acid group, amide group and quaternary ammonium group, these groups are easy to form hydrogen bonds with solvents, which promote the solvent to penetrate into the hydrogel and cause swelling. Water is a strong polar solvent that can form strong hydrogen bonds with hydrophilic groups. Soaking the hydrogel in water can make the hydrogel swell with water. As can be seen from Fig.6, the hydrogel swelled rapidly when the soaking time was within 0~120 min, and the swelling ratio reached 37g/g when 480 min was reached. The swelling hydrogel was added to ethanol, and the hydrogel deswelling rapidly. At 120 min, the water loss rate reached 93.51%, and at 360 min, the dissolution reached equilibrium. This phenomenon is due to the fact that ethanol is a weak polar solvent, which can not completely ionize the sulfonic acid groups in LAD hydrogel. Instead, the ethanol makes positive and negative ions form dipoles, and the interaction between dipoles make the hydrogel volume shrink and lose water (Zeng 2007). When the hydrogel dissolved in ethanol is re-added to the water, the swelling phenomenon will occur again, indicating that the hydrogel has good reversibility. By changing the type of solvent, the responsiveness of the hydrogel can be adjusted to achieve the desired effect of the application.

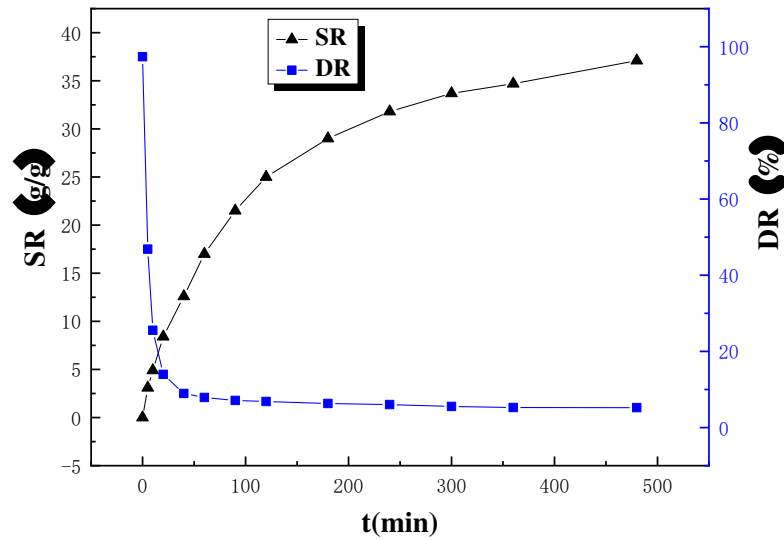
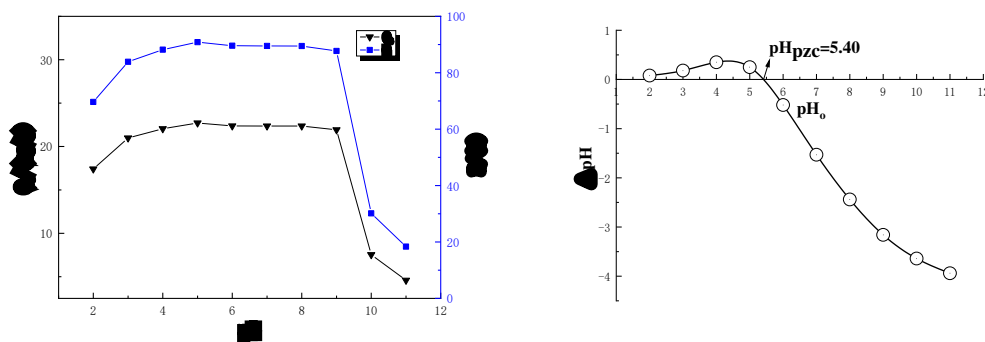


Fig. 6. Swelling/deswelling behavior of LAD hydrogel in water/ethanol

## Effects of adsorption conditions on the adsorption of LAD

### Effect of solution pH

The solution pH value is an important factor affecting the adsorption capacity of the hydrogel adsorbent for dyes, and it is closely related to the surface charge of the adsorbent (Duangkamol et al. 2018). In order to explore the effect of pH on the adsorption process, 0.1 g of dried hydrogel was accurately weighed, and after swelling and equilibrium was placed in a series of 150mL conical bottles, then 50 mL 50mg/L AR 73 solution was added. The range of adjusting solution of pH is 2-11, and the remaining concentration of AR 73 in the solution was determined after oscillation and adsorption in water-bathing constant temperature vibrator at 30 °C for 1h. The result was shown in Fig. 7.



**Fig. 7** Effect of pH on adsorption capacity and adsorption rate of AR 73

**Fig. 8** Isoelectric point of LAD hydrogel adsorbent

As shown in Fig.7, the adsorption capacity and adsorption rate were gradually increased when the solution pH was between 2 and 5, and reached the maximum at pH=5, and the adsorption capacity and adsorption rate were 22.72mg/g and 90.86%, respectively. When the solution pH was in the range of 5 to 9, the adsorption capacity and adsorption rate gradually decreased slowly and decreased sharply with the increment of pH. By measuring the isoelectric point analysis of LAD hydrogel, it can be known that the isoelectric point of LAD hydrogel is  $pH_{pzc}=5.40$  (Fig.8) .It can be concluded that when  $pH < 5.40$ , the surface of LAD was positively charged. The nitrogenous groups (such as  $-NH_2$ ,  $-CH_2-N^+(CH_3)_3$ ) in the hydrogel were protonated under acidic conditions, and AR 73 was adsorbed by electrostatic gravitation, hydrogen bond and ion exchange. Meanwhile, the nitrogen atom has five valence electrons, and its lone pair of electrons can interact with pollutants to achieve the purpose of adsorption (Godiya et al. 2020). In addition, some AR 73 molecules interacted with benzene ring and hydrophobic groups on the surface of LAD by van der Waals force to induce dipoles and attract each other (Wang et al. 2018), thus increasing the adsorption capacity. On the contrary, when the pH exceeded  $pH_{pzc}$ , the LAD surface was negatively charged. With the increase of pH, the oxygen-containing groups on the surface of LAD (such as sulfonic acid groups, methoxy groups, alcohol hydroxyl groups) and nitrogen and sulfur elements in AR 73 molecules gradually deprotonated. Due to electrostatic repulsion, AR 73 molecules were difficult to be adsorbed on the surface of LAD, leading to a decrease in adsorption capacity. And with the increase of pH, the chromaticity of AR 73 solution also increases. Therefore, it is ideal to choose the solution pH near the isoelectric point of LAD hydrogel.

### **Effect of adsorption time**

Adsorption rate is an important parameter of adsorption process. Accurately weigh 0.1 g of the dried hydrogel and placed it in a 150mL conical flask with stopper after swelling and equilibrium. After then, 50 mL of 50mg/LAR 73 solution was added to adjust the pH to 5.0, and oscillation and adsorption in water-bathing constant

temperature vibrator at 30 °C. At intervals, the absorbance of the supernatant was measured, and the concentration of the remaining solution was calculated. The adsorption of LAD hydrogel adsorbent to AR 73 at different time was investigated, and the results were shown in Fig. 9 (a,b).

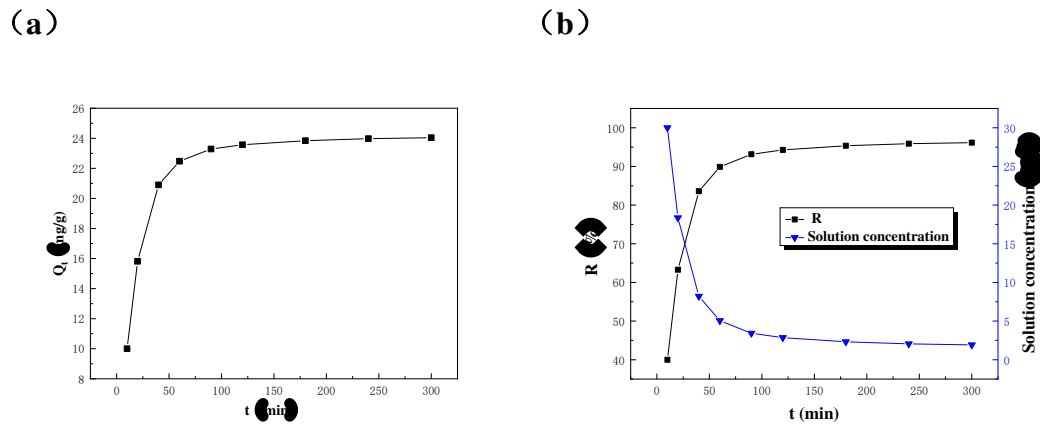


**Fig. 9** (a) Relationship between adsorption capacity and time (b) Effects of time on the adsorption

As shown in Fig. 9 (a,b), the adsorption capacity and adsorption rate of LAD hydrogel to AR 73 increase with the increase of adsorption time. In the range of adsorption time from 0~40min, the adsorption capacity and adsorption rate increased sharply, which were 20.9mg/g and 83.6%, respectively. At this time, the remaining concentration of the solution was only 8.2mg/L. This shows that it belonged to the stage of fast adsorption in this period of time. The adsorption capacity and adsorption rate increase slowly within 40~120 min, this stage belonged to the slow adsorption stage. At 120min, the adsorption capacity and adsorption rate reached 23.57mg/g and 94.28%, respectively. After 120min, it basically reached the stage of dynamic adsorption equilibrium. Therefore, the adsorption equilibrium time selected in the subsequent experiments is 120 min.

### Effect of adsorbent dosage

Different amounts of LAD hydrogel adsorbents were added to 50mL of the solution with an initial concentration of 50mg/L AR 73, and the pH was adjusted to 5.0. After oscillating adsorption in water-bathing constant temperature vibrator at

30 °C for 2 h, the absorbance value was measured, and the adsorption capacity and adsorption rate were calculated. The results were shown in Fig. 10.

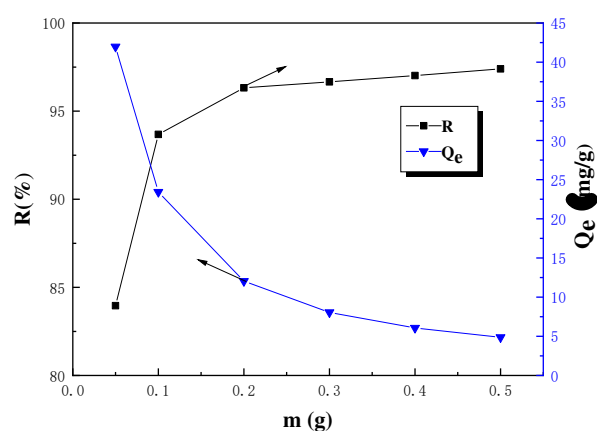


**Fig. 10** Effect of initial concentration of AR 73 solution on adsorption properties

As can be seen from Fig.10, with the increase of the amount of LAD hydrogel adsorbent, the adsorption capacity decreased rapidly, while the adsorption rate increased rapidly at first and then tended to equilibrium. When the hydrogel was 0.1g, the adsorption capacity and adsorption rate reached 23.42mg/g and 93.68%, respectively. After that, with the increase of the dosage of hydrogel, the adsorption capacity will be greatly reduced, and the adsorption rate will only increase slightly. When the hydrogel dosage was 0.5g, the adsorption rate reached 97.4%, while the adsorption amount was only 4.87mg/g. When the hydrogel dosage was 0.5g, the adsorption rate reached 97.4%, while the adsorption amount was only 4.87mg/g. This is because when the dosage of LAD hydrogel gradually increases, the number of corresponding active adsorption sites also increases, so that more dye molecules can be absorbed and the adsorption rate gradually increases. However, the mass concentration of dyes in the solution is certain, and when the dosage increases, the dye adsorption per unit mass of LAD hydrogel adsorbent becomes less, so that the utilization of the active adsorption site is not complete, thus the adsorption capacity decreases (Wu et al. 2019). Considering the adsorption capacity and adsorption rate, the dosage of LAD hydrogel adsorbent is 0.1g in the later experiment.

### **Effect of initial concentration**

In order to investigate the effect of initial concentration of AR 73 on the adsorption performance of LAD hydrogel adsorbent, 0.1g hydrogel adsorbent was accurately weighed in swelling equilibrium and placed in a series of conical flasks. Then add different concentrations of 50mL AR 73 solution. Adjusting the pH=5.0, to oscillate and adsorb in water-bathing constant temperature vibrator at 30 °C for 2 h, and the results were shown in Fig. 11.

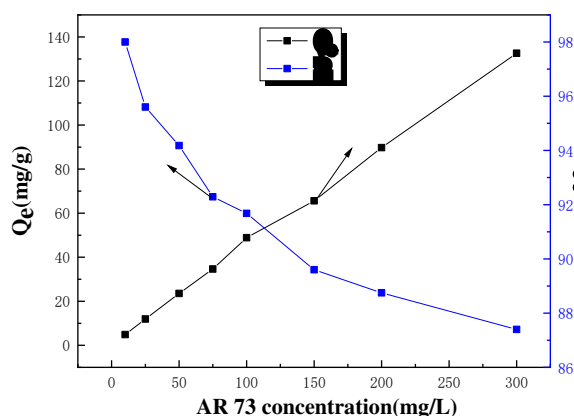


**Fig. 11** Effect of initial concentration of AR 73 solution on adsorption properties

As Fig. 11 shown that with the increase of AR 73 concentration, the adsorption capacity increased, while the adsorption rate decreased. This is because the dosage of the hydrogel adsorbents are constant, so the active adsorption sites on the surface also remain unchanged. As the concentration of AR 73 increased, the active site of the adsorbent was surrounded by more AR 73 molecules, thereby promoting the increase of adsorption capacity. When the initial concentration of AR 73 was low, the dye molecules of AR 73 could reach the adsorption site smoothly, and with the increase of AR 73 concentration, the active adsorption site was occupied by dye molecules (Xu et al. 2015). The increase of AR 73 concentration on the hydrogel surface led to the decrease of the concentration difference of AR 73 between the hydrogel surface and the solution, and the decrease of driving force led to the slow increase of adsorption capacity. When the adsorption site is filled with AR73 dye molecules, the adsorption reaches saturation. After that, even if the AR73 concentration continues to increase, the adsorption capacity will no longer increase, and the adsorption rate will continue to decrease (Chen et al. 2014).

## Effect of temperature

In the process of adsorption, temperature is a crucial factor. As shown in Fig.12, with the increase of temperature, the adsorption capacity and adsorption rate of LAD hydrogel adsorbent for AR 73 decreased slightly. The increase of temperature may also lead to more intense irregular movement of molecules and increase the cross-linking of macromolecules in the hydrogel. When the dye entered the internal pores of the hydrogel sphere, it is more likely to be blocked, and the molecular weight of the dye entering the LAD hydrogel adsorbent decreases (Shahin et al. 2018). It led to the decrease of adsorption capacity and adsorption rate. At 30 °C, the adsorption capacity and adsorption rate were 47.59 mg/g and 95.18%, respectively. In addition, with the increase of temperature, the hydrogel may desorb, which will also reduce the adsorption capacity and adsorption rate of AR 73. Therefore, when the AR 73 was adsorbed and decolorized, the temperature should be controlled at low temperature as far as possible.

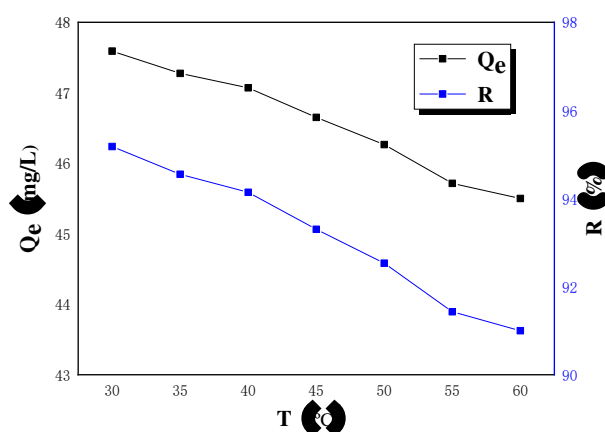


Fig. 12 Effect of temperature on adsorption properties

## Study on adsorption Kinetics

The adsorption rate is one of the important indexes to evaluate the practicability of adsorbents. The study of adsorption kinetics are of great significance for understanding the adsorption rate and analyzing the adsorption mechanism. In order to analyze the adsorption rate of LAD hydrogel adsorbent to AR 73 at different concentrations and explore the adsorption mechanism, the experimental data were fitted by pseudo-first-order kinetic model (Javadian et al. 2014), pseudo-second-order

kinetic model (Ansari et al. 2011) and internal diffusion model (Nethaji and Sivasamy 2011), respectively. The linear equations of the three dynamics models were shown in equations (5) ~ (7).

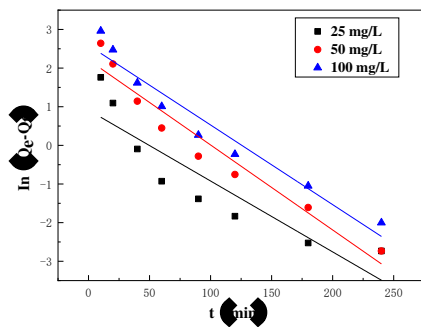
$$\ln(Q_e - Q_t) = \ln Q_t - k_1 t \quad (5)$$

$$\frac{t}{Q_t} = \frac{1}{k_2 Q_e^2} + \frac{t}{Q_e} \quad (6)$$

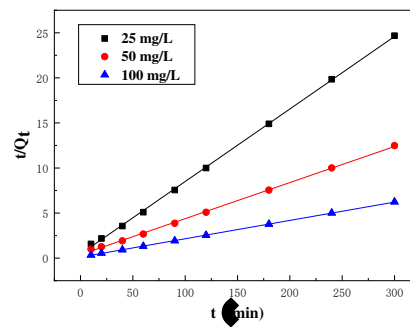
$$Q_t = k_1 t^{\frac{1}{2}} + P \quad (7)$$

Where  $t$  (min) is the adsorption time;  $Q_t$  (mg/g) and  $Q_e$  (mg/g) are the adsorption amount of dye at equilibrium and at time  $t$ , respectively;  $k_1$  ( $\text{min}^{-1}$ ),  $k_2$  ( $\text{g} \cdot \text{mg}^{-1} \cdot \text{min}^{-1}$ ), and  $k_i$  ( $\text{mg} \cdot \text{g}^{-1} \cdot \text{min}^{-0.5}$ ) are all rate constants;  $P$  is a constant related to the thickness of the boundary layer. The linear fitting results and kinetic parameters of the three models were shown in Fig. 13 and Tables 1 and 2, respectively.

(a)



(b)



(c)

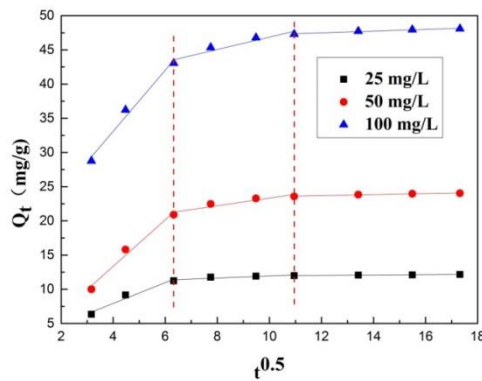


**Fig. 13** Kinetic models of acid red 73 at different concentrations:(a) pseudo-first-order kinetic model, (b) pseudo-second-order kinetic model, (c) Internal diffusion model

According to Table 1, the correlation coefficient ( $R^2 > 0.999$ ) of the pseudo-second-order kinetic model was significantly higher than that of the pseudo-first-order kinetic model when the LAD hydrogel adsorbent adsorbed AR 73 at three different concentrations, and the calculated equilibrium adsorption capacity ( $Q_e$ ) was also closer to the measured value. This shown that the adsorption of AR 73 by LAD conformed to the pseudo-second-order kinetic adsorption model. The pseudo-second-order kinetic model assumed that the adsorption rate was determined by the square of the number of adsorption vacancies not occupied on the adsorbent surface, and the adsorption process was controlled by the chemical adsorption mechanism (Shahin et al. 2018). This chemical adsorption may be caused by the electrostatic interaction between the quaternary ammonium group contained in LAD hydrogel adsorbent and AR 73. Similar conclusions have been obtained in the research of other researchers (Xu et al. 2015; Zhang 2018a). Fig.13c shown that the P value obtained by piecewise fitting of the internal diffusion model in three time periods was not 0, that is, the straight line did not pass through the origin, indicating that internal diffusion was not the only step in the whole adsorption process (Sun et al. 2013). There may also be the effect of surface adsorption and membrane diffusion on the adsorption rate.

**Table 1** The parameters of dynamic models of acid red 73 at different concentrations

$C_0$ mg/L	$Q_{e,exp}$ mg/g	Pseudo-first-order dynamics model			Pseudo-second order dynamic model		
		$k_1/min^{-1}$	$Q_{e,1}/mg \cdot g^{-1}$	$R^2$	$k_2/(g \cdot mg^{-1} \cdot min^{-1})$	$Q_{e,2}/mg \cdot g^{-1}$	$R^2$
25	12.16	0.01834	2.489	0.7953	0.01420	12.43	0.9996
50	24.06	0.02199	9.114	0.9371	0.00423	24.98	0.9991
100	48.09	0.02061	13.31	0.9414	0.00347	49.19	0.9998

(Note:  $Q_{e,exp}$  is the equilibrium adsorption capacity of the actual experiment, and  $Q_{e,1,2}$  is the equilibrium adsorption capacity calculated by the second-order rate equation.)

**Table 2** The parameters of internal diffusion model of acid red 73 at different concentrations

C <sub>0</sub> / mg/L	Internal diffusion dynamics model								
	0~40min			40~120min			120~300min		
	K <sub>i</sub> /(mg·g <sup>-1</sup> ·min <sup>-0.5</sup> )	P	R <sup>2</sup>	K <sub>i</sub> /(mg·g <sup>-1</sup> ·min <sup>-0.5</sup> )	P	R <sup>2</sup>	K <sub>i</sub> /(mg·g <sup>-1</sup> ·min <sup>-0.5</sup> )	P	R <sup>2</sup>
25	1.521	1.85	0.93	0.152	10.42	0.75	0.023	11.74	0.93
50	3.399	-0.24	0.96	0.562	17.713	0.84	0.074	22.79	0.93
100	4.464	15.24	0.96	0.903	37.83	0.88	0.12	45.99	0.94

According to the above analysis, the pseudo-second-order kinetic model was used to study the adsorption process of LAD hydrogel adsorbent on AR 73 at different temperatures. The linear fitting results and kinetic parameters of the experimental data were shown in Fig.14 and Table 3, respectively.

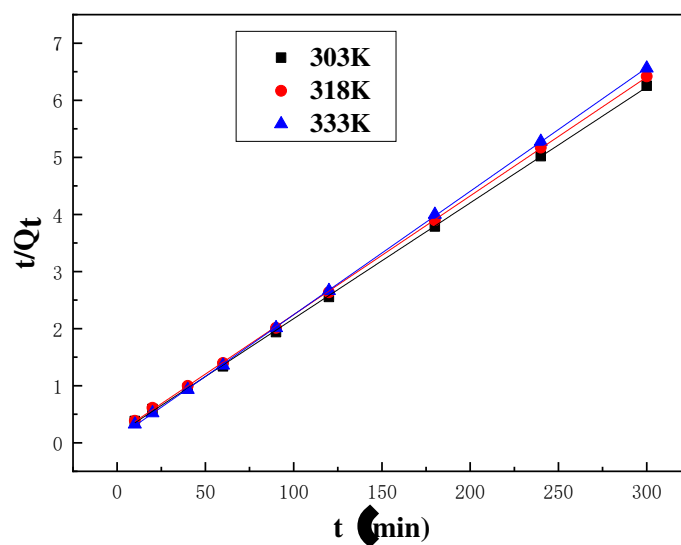


**Fig. 14** Pseudo-second-order kinetic model of AR 73 at different temperatures

It can be seen from Table 3 that with the increase of temperature, the adsorption capacity of LAD to AR 73 decreased, and the adsorption rate  $K_2$  also decreased. Therefore, high temperature was not conducive to adsorption. After then, the apparent activation energy  $E_a$  of LAD hydrogel adsorbent was calculated according to Arrhenius equation. Using  $\ln K_2$  to draw the graph of  $1/T$ , the straight line equation was  $-\ln K_2 = -0.3008/T + 6.87131$  ( $R^2 = 0.95644$ ), and then the  $E_a = 2.501$  kJ/mol was calculated from the slope. In general, the apparent activation energy of physical adsorption and chemical adsorption takes 40 kJ/mol as a limit (Karthik and Meenakshi 2014). When it is lower than 40 kJ/mol, it is dominated by physical

adsorption, on the contrary, it is dominated by chemical adsorption. Therefore, the adsorption of AR 73 by LAD hydrogel adsorbent may be an adsorption process dominated by physical adsorption.

**Table 3** The parameters of pseudo-second-order dynamic model of AR 73 at different temperatures

C <sub>0</sub> / mg/L	T/ K	Q <sub>e.exp</sub> mg/g	Pseudo-second order dynamic model		
			k <sub>2</sub> / (g • mg <sup>-1</sup> • min <sup>-1</sup> )	Q <sub>e.2</sub> /mg • g <sup>-1</sup>	R <sup>2</sup>
100	303	47.98	0.00281	49.31	0.99981
	318	46.84	0.00265	48.05	0.99990
	333	45.73	0.00257	46.25	0.99993

### Study on isothermal adsorption

Adsorption isotherm is an important method to study the adsorption properties and surface properties of adsorbent materials. Langmuir (Sharma et al. 2018), Freundlich (Alidokht et al. 2011) and Temkin (Ansari et al. 2011) models are three common adsorption isotherms, which describe monolayer adsorption on uniform surface, multi-layer adsorption on inhomogeneous surface and adsorption between molecules in the adsorption process. The linear equations of the three adsorption isotherm models were shown in equations (8) ~ (10).

$$\frac{C_e}{Q_e} = \frac{1}{Q_m K_L} + \frac{C_e}{Q_m} \quad (8)$$

$$\ln Q_e = \ln K_F + \frac{1}{n} \ln C_e \quad (9)$$

$$Q_e = \beta \ln \alpha + \beta \ln C_e \quad (10)$$

Where C<sub>e</sub> (mg/L) is the concentration of AR 73 in the solution at adsorption equilibrium, Q<sub>m</sub> (mg/g) is the saturated adsorption capacity; K<sub>L</sub> (L • mg<sup>-1</sup>) is the adsorption coefficient; K<sub>F</sub> and n are constants, when n > 1, the adsorption is easy, and α and β are constants.

Under the condition of 0.1g LAD dosage, pH 5.0 and adsorption time of 4h, the adsorption characteristics of LAD on AR 73 were investigated at different

temperatures(303K, 318K, 333K). The three adsorption isotherms were shown in Fig. 15, and the data fitting results were shown in Table 4.

It can be seen from Table 4 that the correlation coefficients ( $R^2 > 0.96$ ) fitted by Langmuir model were better than the Freundlich and Temkin models under three temperature conditions. This shown that the adsorption process of LAD on AR 73 conformed to the Langmuir adsorption model. It was inferred that the adsorption of AR 73 by LAD belonged to monolayer adsorption. In Langmuir isothermal adsorption, the adsorption capacity( $Q_e$ ) and adsorption coefficient ( $K_L$ ) both decreased with the increase of temperature, indicated that low temperature was favorable for adsorption. When the temperature was 303K, the maximum adsorption capacity of LAD hydrogel adsorbent on AR 73 was 409.84mg/g.

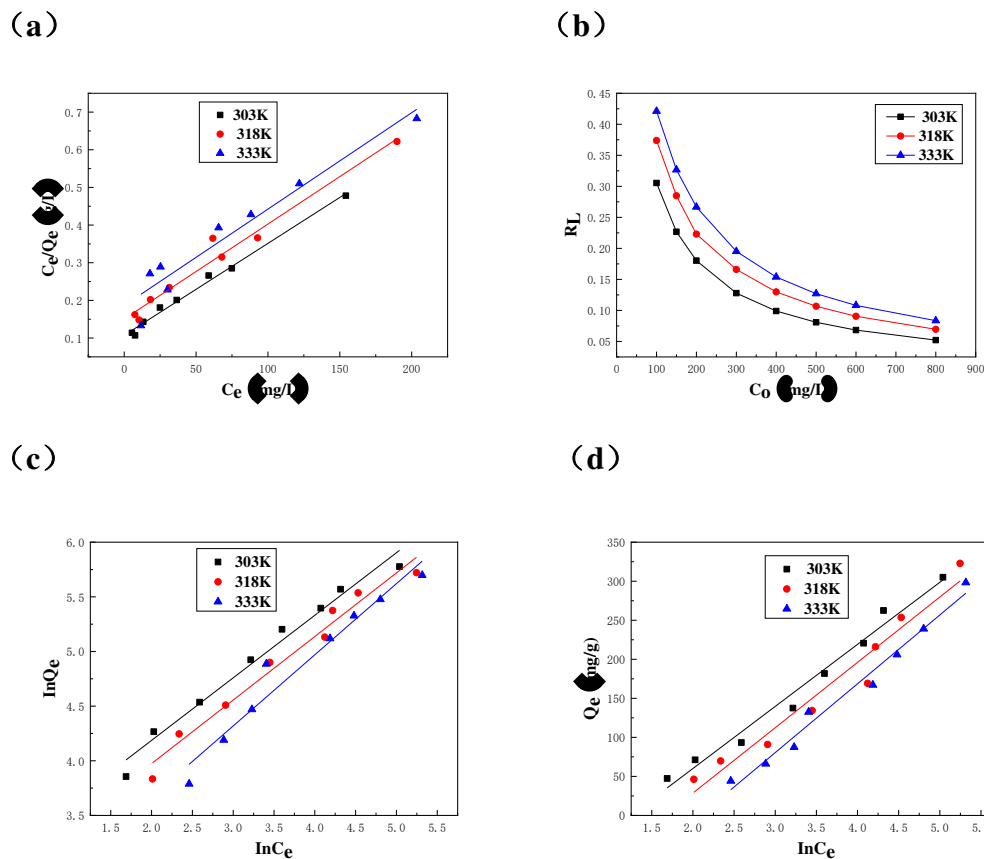


**Fig. 15** Adsorption isotherms at different temperatures: (a) Langmuir; (b) Relationship between  $R_L$  and  $C_0$  at different temperatures; (c) Freundlich; (d) Temkin

**Table 4** The parameters of isothermal adsorption model at different temperatures

T/	Langmuir isothermal adsorption model	Freundlich isothermal adsorption model	Temkin isothermal adsorption model
----	--------------------------------------	--	------------------------------------

K	Q <sub>m</sub> / mg·g <sup>-1</sup>	K <sub>L</sub> /L· mg <sup>-1</sup>	R <sup>2</sup>	K <sub>F</sub> / mg·g <sup>-1</sup>	n	R <sup>2</sup>	α	β	R <sup>2</sup>
303	409.84	0.0227	0.99013	20.945	1.747	0.97597	0.288	79.519	0.97760
318	396.83	0.0167	0.96658	16.621	1.719	0.96547	0.191	83.715	0.94713
333	390.63	0.0137	0.96585	10.651	1.536	0.94525	0.124	88.154	0.95658

$R_L$  is a dimensionless separation factor defined by Langmuir model, which can be used to judge the difficulty of adsorption. The expression was as follows (Mohammed et al. 2018).

$$R_L = \frac{1}{1 + K_L C_0} \quad (11)$$

Where  $C_0$  (mg/L) is the initial concentration of the solute. The value of  $R_L$  between 0 and 1 is easy to adsorb,  $R_L=1$  is reversible, and when  $R_L > 1$ , the adsorption is not easy.

Fig.15 b shown that the values of  $R_L$  were all between 0 and 1 at different temperatures, indicated that the adsorption process of Langmuir model was easy to carry out. In addition, the  $n$  values calculated by Freundlich model were all greater than 1, which also reflected that the adsorption process was easy to occur. This shown that the synthesized LAD hydrogel adsorbent was easy to adsorb AR 73 and is a kind of adsorption material with excellent adsorption properties.

### Study on adsorption thermodynamics

In order to further study the thermodynamic properties of adsorption, the Gibbs free energy change ( $\Delta G$ , kJ/mol) and enthalpy change ( $\Delta H$ , kJ/mol) and entropy change ( $\Delta S$ , J/mol·K) were calculated by van der Hoff and Gibbs-Helmhotz equations (Mao et al. 2018) at different temperatures. The specific formula are as follows:

$$K_L = \frac{Q_e}{C_e} \quad (12)$$

$$\Delta G = -RT \ln K_L \quad (13)$$

$$\ln K_L = \frac{\Delta S}{R} - \frac{\Delta H}{RT} \quad (14)$$

Where  $R$  is the gas constant,  $8.314\text{J/mol}\cdot\text{K}$ ;  $T$  (K) is the absolute temperature;  $K_L$  (L/g) is the equilibrium constant.

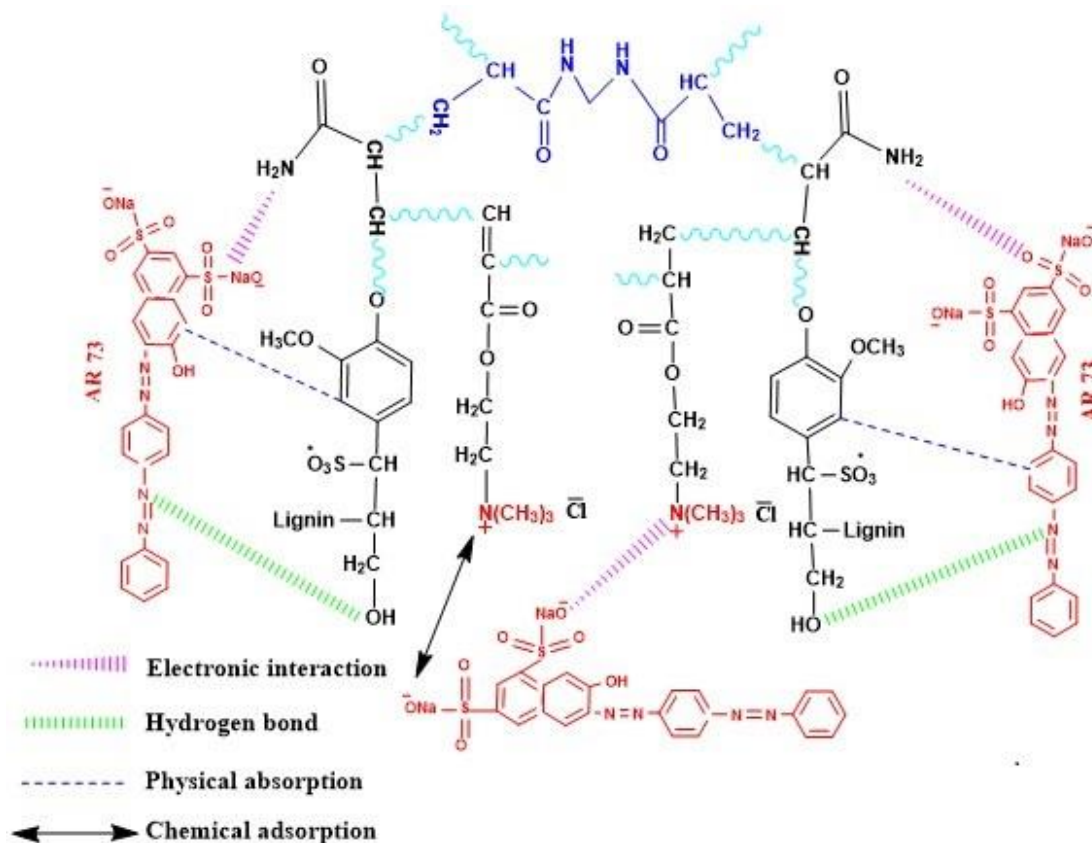
At different temperatures,  $Q_e$  can be linearly fitted by  $\ln(Q_e/C_e)$ , and the intercept is  $\ln K_L$ . After then, substituting  $K_L$  into equation (13) to calculate  $\Delta G$ . The slope and intercept of the line obtained by plotting  $1/T$  by  $\ln K_L$  are  $\Delta H$  and  $\Delta S$ , and the results were shown in Table 5.

As Table 5 shown that the  $\Delta G$  of the LAD hydrogel adsorbent for AR 73 adsorption process was less than 0, indicating that the adsorption process was spontaneous. And with the increase of temperature, the  $\Delta G$  force became larger and the adsorption driving force weakened, indicated that high temperature was not conducive to adsorption.  $H < 0$ , the adsorption process belongs to exothermic, and the low temperature was benefitted to the adsorption, which was consistent with the Langmuir adsorption process.  $\Delta S < 0$ , it shown that the adsorption process was a process of decreasing entropy.

**Table 5** Adsorption thermodynamic parameters at different temperatures

T/K			$\Delta H$ ( $\text{kJ}\cdot\text{mol}^{-1}$ )	$\Delta S$ ( $\text{J}\cdot\text{mol}^{-1}\cdot\text{K}^{-1}$ )
303	318	333		
$\Delta G$ ( $\text{kJ}\cdot\text{mol}^{-1}$ )				
-6.247	-5.564	-4.494	-23.640	-57.183

Studies have shown (Berizi et al. 2016; Mao et al. 2018) that when the absolute value of  $\Delta G$  is less than  $20\text{ kJ}\cdot\text{mol}^{-1}$ , the adsorption is physical adsorption; when the absolute value of  $\Delta H$  is within the range of  $2\sim 29\text{kJ}/\text{mol}$ , the force between the adsorbent and the solute is dominated by hydrogen bonding. It can be seen from Table 5 that the absolute value of  $\Delta G$  during the adsorption process of the LAD hydrogel adsorbent on AR 73 was  $4.494\sim 6.247\text{ kJ}\cdot\text{mol}^{-1}$ , and the absolute value of  $\Delta H$  was  $23.640\text{ kJ}\cdot\text{mol}^{-1}$ . It shown that there was hydrogen bond in the adsorption process of LAD on AR 73 in addition to physical adsorption. Therefore, combined with the above analysis in this paper, the adsorption mechanism of LAD hydrogel adsorbent on AR 73 ( Fig.16) is the result of electrostatic interaction, physical and chemical adsorption and hydrogen bonding interaction.



### LS-g-P(AM-co-DAC) Hydrogel

Fig. 16 The adsorption mechanism of LAD hydrogel adsorbent

### Regeneration of LAD

Using the nitric acid solution of 0.1mol/L as desorption agent, the LAD hydrogel adsorbent after adsorption-desorption of AR73 was recycled for 10 times, the adsorption rate was still more than 90%, indicating that LAD hydrogel adsorbent has good recycling ability and is a good recyclable hydrogel adsorbent.

### Conclusions

In this paper, a biomass LAD hydrogel adsorbent with high water absorption and adsorption properties was successfully synthesized by free radical graft copolymerization. The swelling ratio reached 37g/g within 480min, and the water loss rate reached 93.51% within 2h in ethanol solvent, showing good swelling and deswelling properties. Under the conditions of 0.1g, pH=5.0 and 30 °C, the adsorption of AR 73 solution with initial concentration of 100mg/L by LAD reached equilibrium for 2 h, and the equilibrium adsorption capacity and adsorption rate were 47.59mg/g and 95.18%, respectively.

Through data fitting, it was found that the adsorption of LAD to AR 73 conformed to the Langmuir isotherm adsorption model, and was a monolayer adsorption, with the maximum adsorption capacity of 409.84mg/g; The adsorption kinetics conformed to the pseudo-second-order kinetic, and the adsorption activation energy is 2.501 kJ/mol. The adsorption of AR 73 by LAD was a process of spontaneous exothermic and entropy reduction. Furthermore, the adsorption mechanism of LAD is mainly electrostatic interaction, which was also the result of the combination of physical and chemical adsorption and hydrogen bond. In sum, LAD hydrogel adsorbent has a significant adsorption effect on AR 73, and can be used as an efficient and recyclable biomass adsorbent for the treatment of anionic dye wastewater.

**Authors' contribution** Shuxia Wei: conducted experiments and analyzed experimental data, was a major contributor in writing the original manuscript.

Wu Chen: idea for the article, organization, critical feedback and revision, supervision, conceptualization.

Zhiming Tong and Nan Jiang: literature survey, review and editing, data analysis.

Mijia Zhu: co-supervision, editing, conceptualization and data analysis.

### **Funding**

The authors of this work wish to gratefully acknowledge the financial support from the national major special project "Waste Disposal and Technology" of China (No. 2016ZX05040003).

**Data availability** Not applicable.

## **Compliance with ethical standards**

**Ethics approval and consent to participate** Not applicable.

**Consent for publication** Not applicable.

**Competing interests** The authors declare no competing interests.

## **References**

- Ai JY, Li JB, Li K, Yu F, Ma J (2021) Highly flexible, self-healable and conductive poly(vinyl alcohol)/Ti<sub>3</sub>C<sub>2</sub>T<sub>x</sub> MXene film and its application in capacitive deionization. *Chem Eng J* 408:127256
- Alidokht L, Khataee AR, Reyhanitabar A, Oustan S (2011) Cr(VI) Immobilization process in a Cr-Spiked soil by zerovalent iron nanoparticles: optimization using response surface methodology. *Clean Soil Air Water* 39:633–640
- Ansari R, Keivani MB, Delavar AF (2011) Application of polyaniline nanolayer composite for removal of tartrazine dye from aqueous solutions. *J Polym Res* 18:1931-1939
- Berizi Z, Hashemi SY, Hadi M, Azari A, Mahvi AH (2016) The study of non-linear kinetics and adsorption isotherm models for Acid Red 18 from aqueous solutions by magnetite nanoparticles and magnetite nanoparticles modified by sodium alginate. *Water Sci Technol* 74:1235-1242
- Chen DL, Cao ML, Zhang XM, Peng CS, Chen CY (2014) Synthesis and dye adsorptivity of  $\beta$ -cyclodextrin polymer with a novel tricarboxylic acid as crosslinking agent. *Petrochemical Technology* 43:210-215
- Chen TT, Zhang YJ (2019) Research progress in the synthesis of cationic polyacrylamide P(DAC-AM). *Journal of Chemical Engineering of Chinese Universities* 33:1025-1036
- Chen YQ, Chen LB, Bai H, Li I (2013) Graphene oxide-chitosan composite hydrogels as broad-spectrum adsorbents for water purification. *Journal of Materials Chemistry, A Materials for energy and sustainability* 1:1992-2001
- Duangkamol D, Sahori O, Kensuke N, Takehisa O, Hisashi Y, Tetsuya F, Hiroshi T (2018) Preparation of alginate fibers coagulated by calcium chloride or sulfuric acid: Application to the adsorption of Sr<sup>2+</sup>. *J Hazard Mater* 355:154-161
- EI-Zawawy WK (2005) Preparation of hydrogel from green polymer. *Polym Adv Technol* 16:48-54
- Fan J, Zhan HY, Liu MH (2004) Progress in research on lignin-based adsorption material. *Transactions of China Pulp and Paper* 19:181-187

- Feng QH (2012) Synthesis of properties of lignin-containing hydrogels. South China University of Technology
- Feng QH, Chen FG (2011) Lignin-containing hydrogels. *Journal of Cellulose Science and Technology* 19:67-73
- Godiya CB, Ruotolo LAM, Cai WQ (2020) Functional biobased hydrogels for the removal of aqueous hazardous pollutants: current status, challenges, and future perspectives. *J Mater Chem A* 8:21585-21612
- Guo XY, Zhang SZ, Shan XQ (2008) Adsorption of metal ions on lignin. *J Hazard Mater* 151:134-142
- Javadian H, Angaji MT, Naushad M (2014) Synthesis and characterization of polyaniline/ $\gamma$ -alumina nanocomposite: A comparative study for the adsorption of three different anionic dyes. *J Ind Eng Chem* 20:3890-3900
- Karthik R, Meenakshi S (2014) Adsorption study on removal of Cr(VI) ions by polyaniline composite. *Desalin Water Treat* 54:3083-3093
- Lee KE, Morad N, Teng TT, Poh] BT (2012) Development, characterization and the application of hybrid materials in coagulation/flocculation of wastewater: A review. *Chem Eng J* 203:370-386
- Lee WF, Yeh YC (2005) Studies on preparation and properties of NIPAAm/hydrophobic monomer copolymeric hydrogels. *Eur Polym J* 41:2488-2495
- Lu GD, Yan QZ, Su XT, Liu ZQ, Ge CC (2007) Progress of porous hydrogels. *Progress Chemistry* 19:485-493
- Mao XY, Wang L, Gu SQ, Duan YY, Zhu YQ, Wang CY, Lichtfouse E (2018) Synthesis of a three-dimensional network sodium alginate-poly(acrylic acid)/attapulgate hydrogel with good mechanic property and reusability for efficient adsorption of  $\text{Cu}^{2+}$  and  $\text{Pb}^{2+}$ . *Environ Chem Lett* 16:653–658
- Mohammed C, Mahabir S, Mohammed K, John N, Lee KY, Ward K (2018) Calcium alginate thin films derived from sargassum natans for the selective adsorption of  $\text{Cd}^{2+}$ ,  $\text{Cu}^{2+}$ , and  $\text{Pb}^{2+}$  Ions. *Ind Eng Chem Res* 58:1417-1425

- Nethaji S, Sivasamy A (2011) Adsorptive removal of an acid dye by lignocellulosic waste biomass activated carbon: Equilibrium and kinetic studies. *Chemosphere* 82:1367-1372
- Peñaranda A JE, Sabino MA (2010) Effect of the presence of lignin or peat in IPN hydrogels on the sorption of heavy metals. *Polym Bull* 65:495-508
- Rahul D, Aditi K, Divyashri B, Ali M, Amitava M, Ram M, Pavel F (2017) Enzymatic Degradation of Lignin in Soil: A Review. *Sustainability* 9:1163
- Raschip IE, Hitruc EG, Oprea AM, Popescu MC, Vasile C (2011) In vitro evaluation of the mixed xanthan/lignin hydrogels as vanillin carriers. *J Mol Struct* 1003:67-74
- Shahin, Ahmadi, Chinenye, Adaobi, Igwegbe (2018) Adsorptive removal of phenol and aniline by modified bentonite: adsorption isotherm and kinetics study. *Appl Water Sci* 8:170
- Shao L, Qiu JH, Feng HX, Liu MZ, Zhang GH, An JB, Gao CM, Liu HL (2009) Structural investigation of lignosulfonate doped polyaniline. *Synth Met* 159:1761-1766
- Sharma AK, Priya, Kaith BS, Sharma N, Bhatia JK, Tanwar V, Panchal S, Bajaj S (2018) Selective removal of cationic dyes using response surface methodology optimized gum acacia-sodium alginate blended superadsorbent. *Int J Biol Macromol* 124:331-345
- Sun D, Zhang X, Wu Y, Liu T (2013) Kinetic mechanism of competitive adsorption of disperse dye and anionic dye on fly ash. *Int J Environ Sci Technol* 10:799-808
- Sun YJ, Ma YL, Dai JX, Ren SX, Fang GZ (2016) Preparation and characterization of enzymatic hydrolysis lignin-based hydrogel. *Journal of Beijing Forestry University* 38:97-103
- Van de Manakker F, Kroon-Batenburg LMJ, Vermonden T, van Nostrum CF, Hennink WE (2010) Supramolecular hydrogels formed by  $\beta$ -cyclodextrin self-association and host-guest inclusion complexes. *Soft Matter* 6:187-194

- Wang L, Peng CS, Zhang XM, Ji XL, Lu AW, Liu YC (2018) Preparation of carboxymethylated lignosulfonate cross-linked polymer for adsorption toward methylene blue. *Petrochemical Technology* 47:1369-1375
- Wang Y, Wang XM, Xiong J, Wu SW, Ran Z (2020) Analysis of preparation factors of lignin-based hydrogels synthesized by graft-intercalation. *Environmental Chemistry* 39:2217-2226
- Wu J, Zheng H, Zhang F, Zeng RJ, Xing BS (2019) Iron-carbon composite from carbonization of iron-crosslinked sodium alginate for Cr(VI) removal. *Chem Eng J* 362:21-29
- Xu JH, Mu XK, Hong SM, Ye D, Su Y (2015) Adsorption performance of methylene blue dye by lignin-based hydrogel. *Chinese Journal of Environmental Engineering* 9:4877-4882
- You XY, Wang XL, Zhang HJ, Cui KP, Zhang AK, Wang LP, Yadav C, Li XP (2020) Super tough lignin hydrogels with multienergy dissipative structures and ultrahigh antioxidative activities. *ACS Appl Mater Interfaces* 12:39892-39901
- Yu CH, Wang F, Zhang CH, Fu SY, Lucia LA (2016) The synthesis and absorption dynamics of a lignin-based hydrogel for remediation of cationic dye-contaminated effluent. *Reactive and Functional Polymers* 106:137-142
- Yun XJ, Chi MC, Guo CY, Luo B, Wang SF, Min DY (2019) Research Progress in Lignin-based Hydrogels. *China Pulp & Paper* 38:62-67
- Zeng SJ (2007) Fabrication and studies of polyacrylamide/lignosulfonate gel and properties. Donghua University
- Zhang YH (2018a) Preparation and of Novel Composite Adsorption Materials. Xi'an University of Science and Technology
- Zhang ZL (2018b) Preparation of Modified Lignin-based Adsorbent and Its Application in Wastewater Treatment. South China University of Technology

# Figures

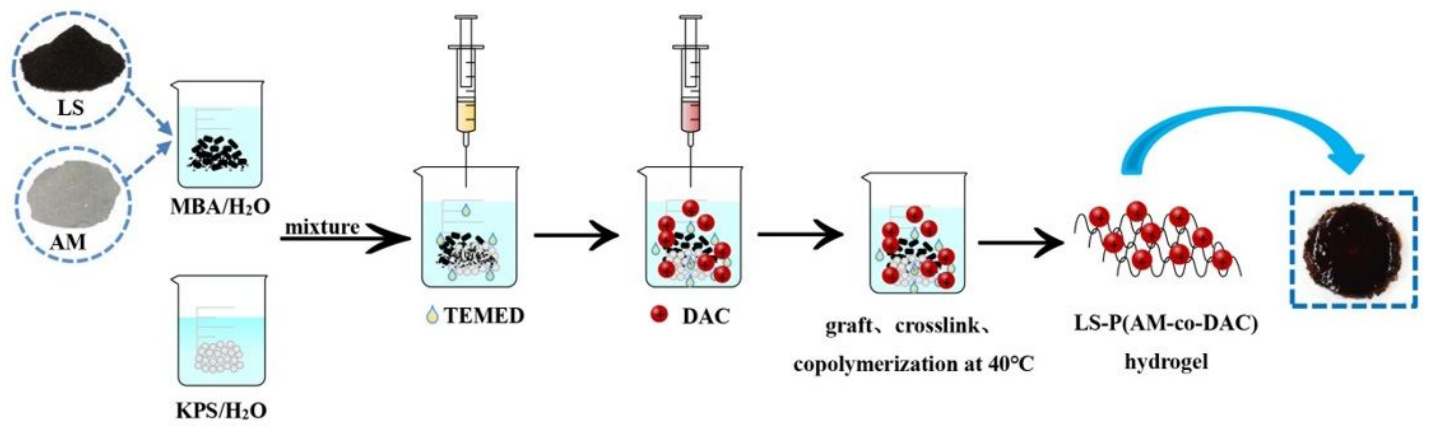


Figure 1

Schematic of the synthesis of LAD hydrogel

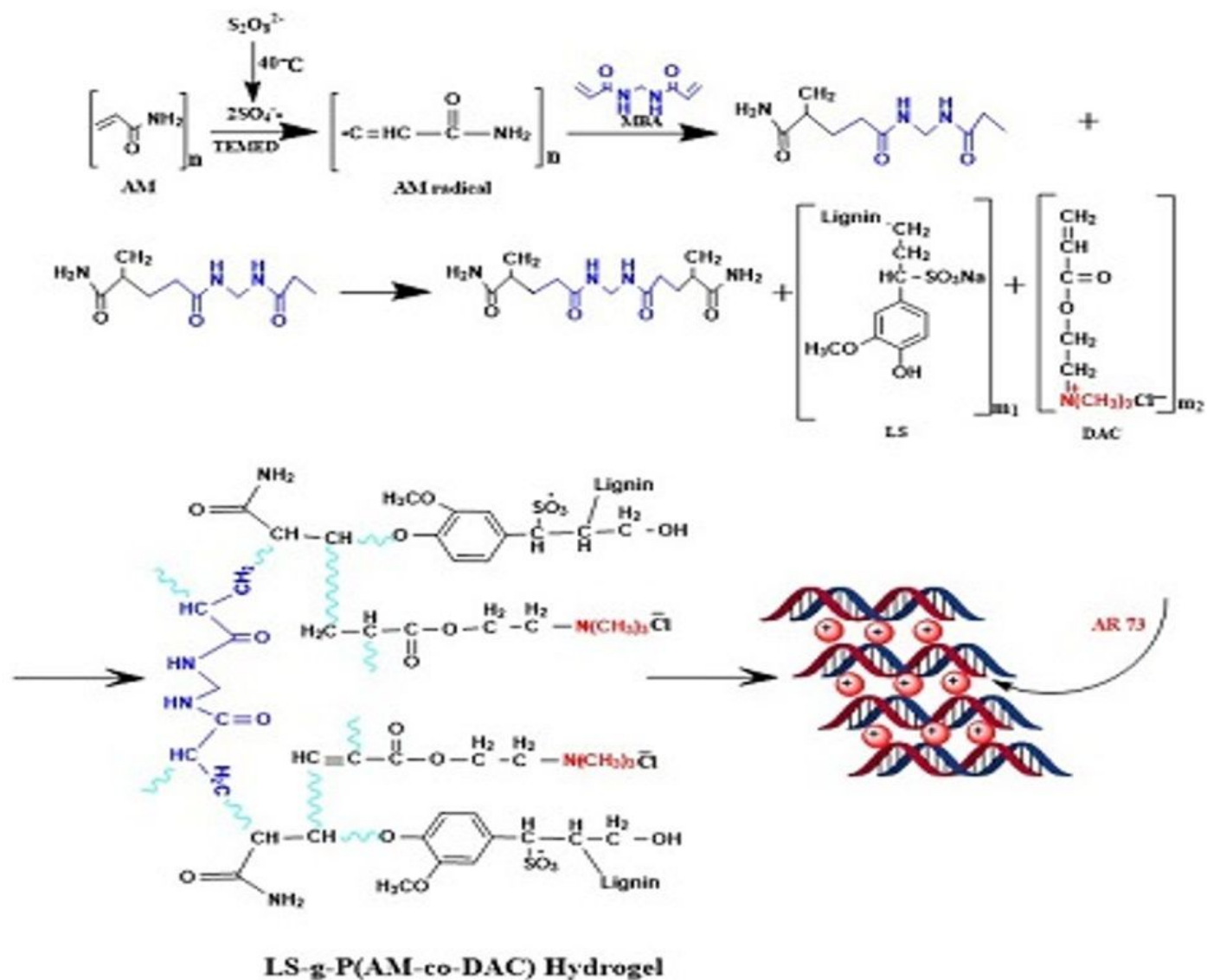


Figure 2

The synthesis mechanism of LAD hydrogel

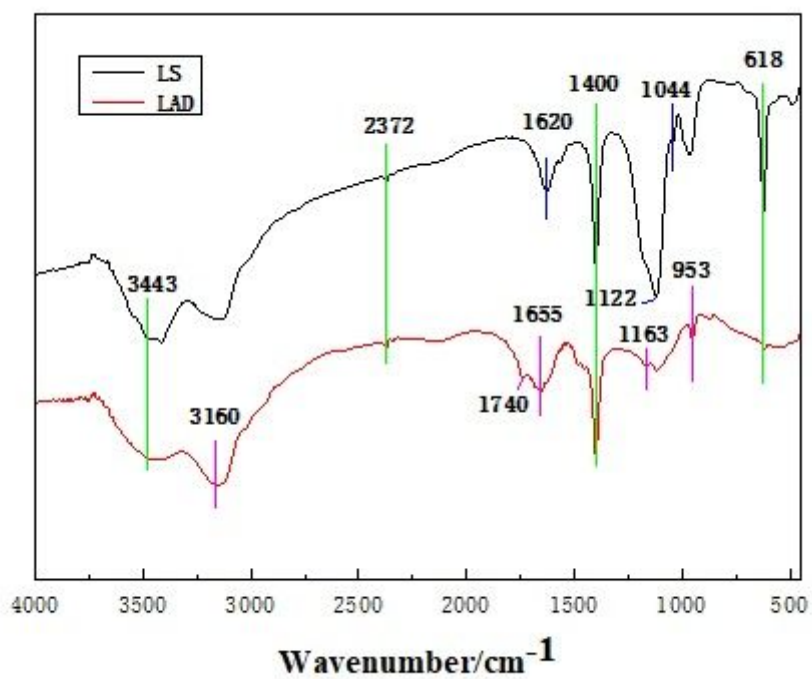


Figure 3

FT-IR spectra of LS and LAD hydrogel adsorbent

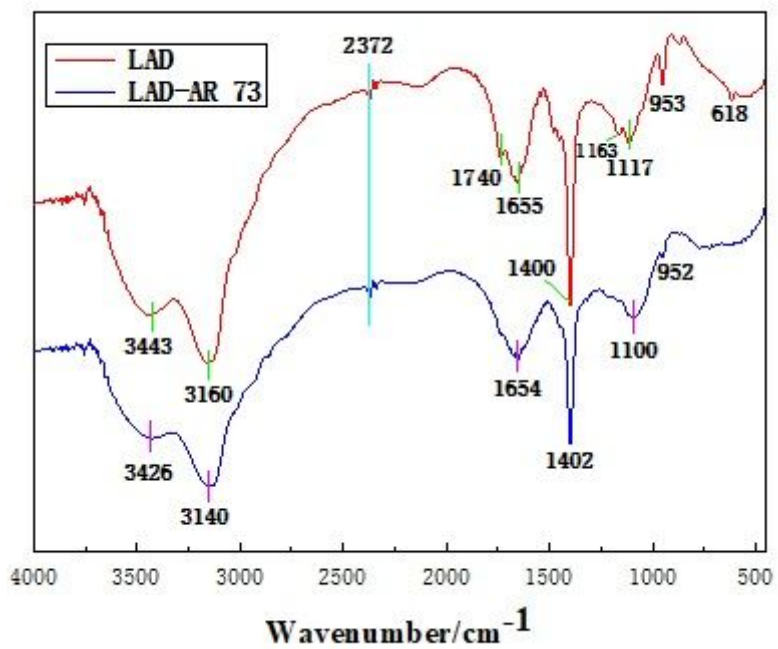


Figure 4

FT-IR spectra of LAD hydrogel adsorbent before and after dye adsorption

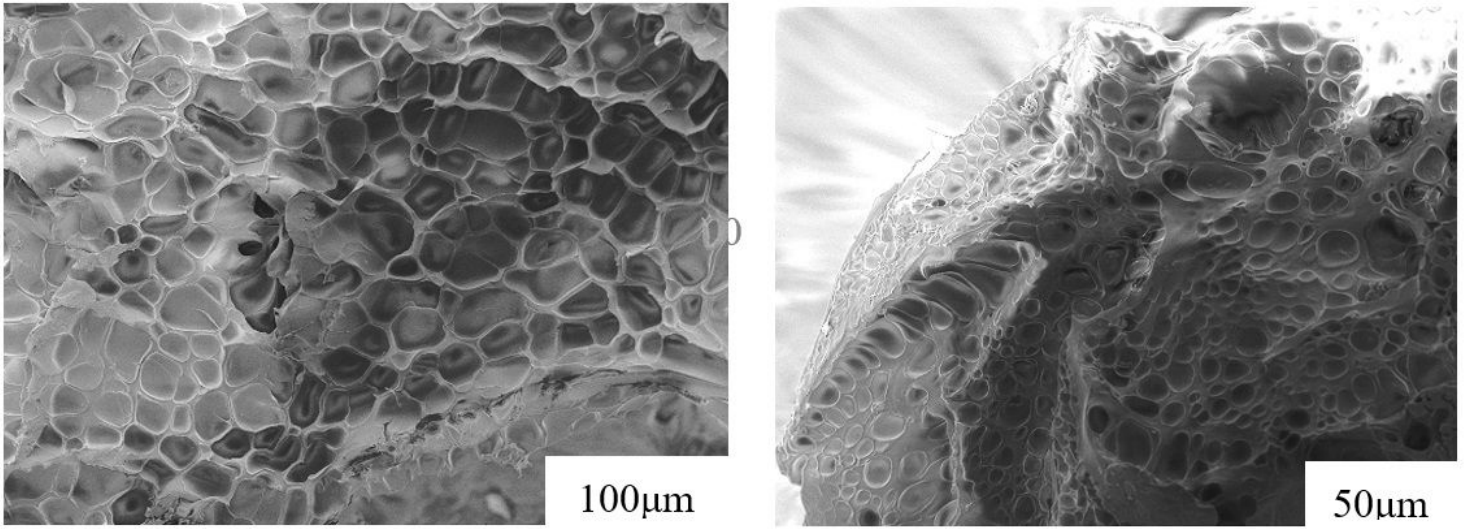


Figure 5

SEM images of LAD hydrogels at different magnification

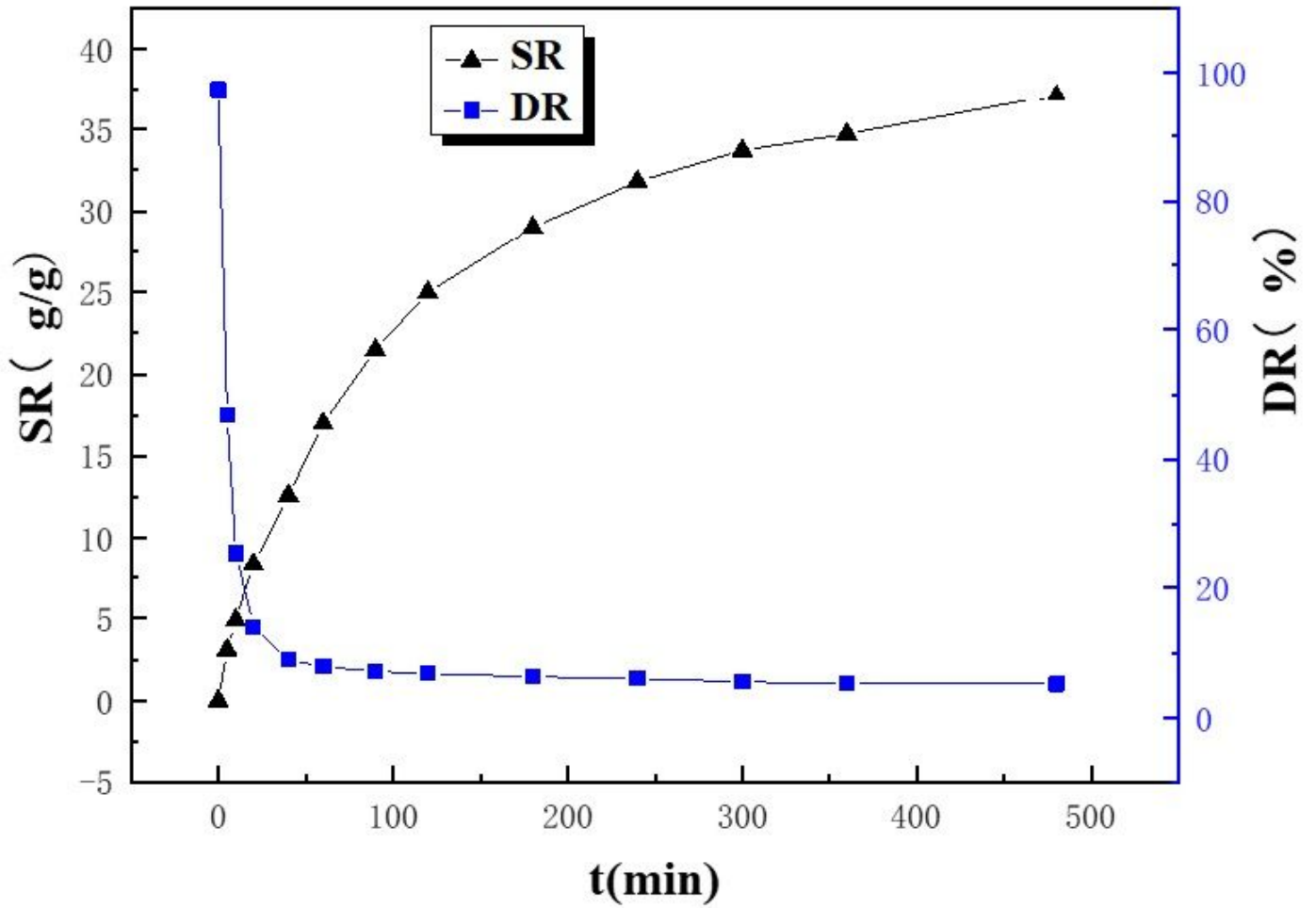


Figure 6

## Swelling/deswelling behavior of LAD hydrogel in water/ethanol

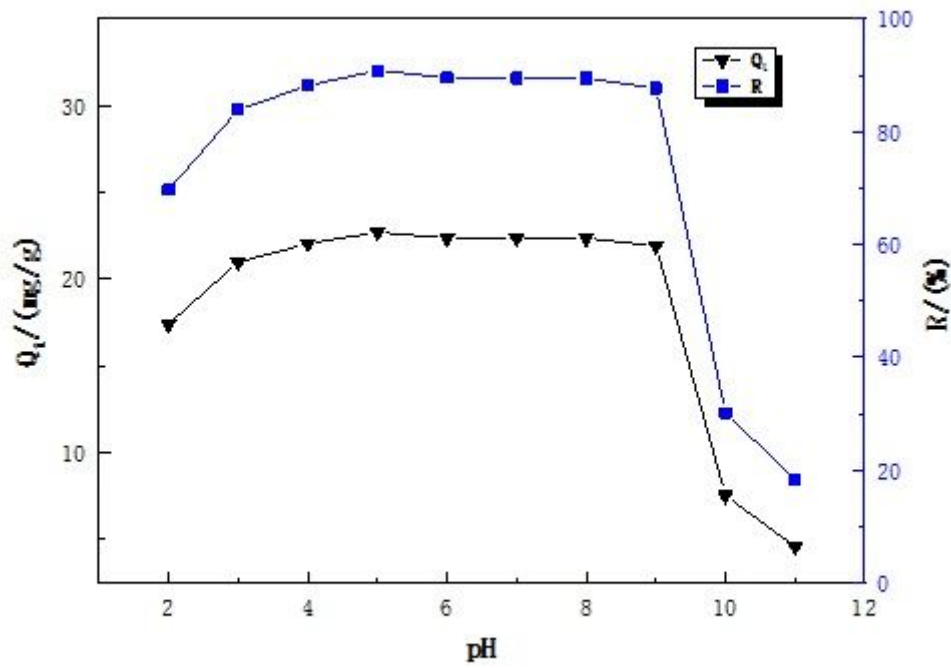


Figure 7

Effect of pH on adsorption capacity and adsorption rate of AR 73

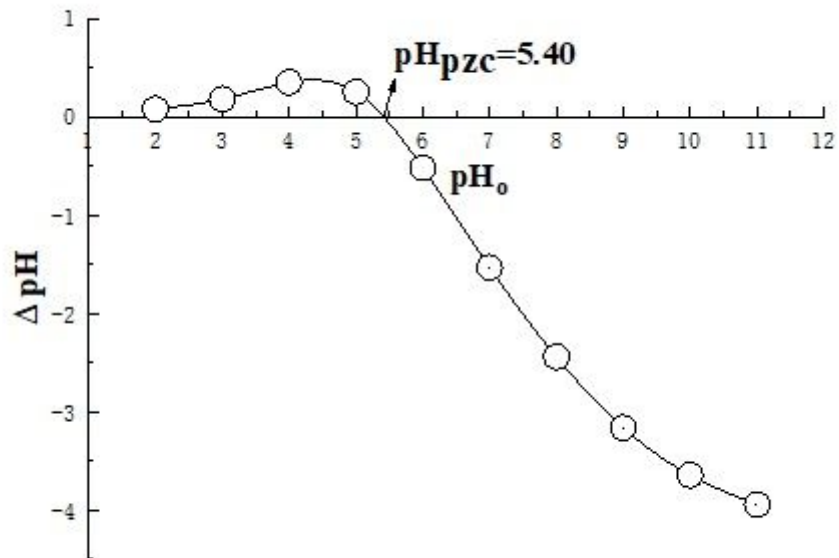
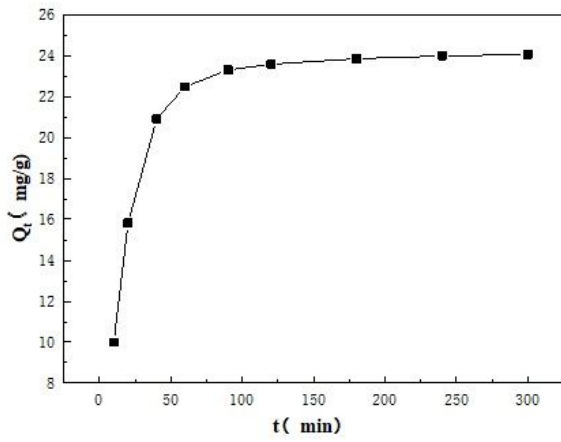


Figure 8

Isoelectric point of LAD hydrogel adsorbent

(a)



(b)

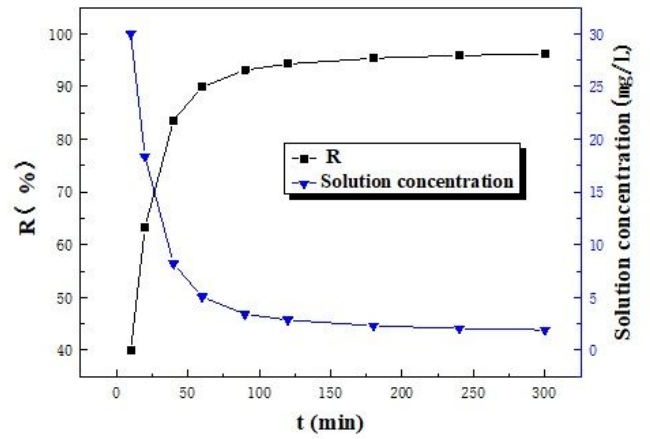


Figure 9

(a) Relationship between adsorption capacity and time (b) Effects of time on the adsorption

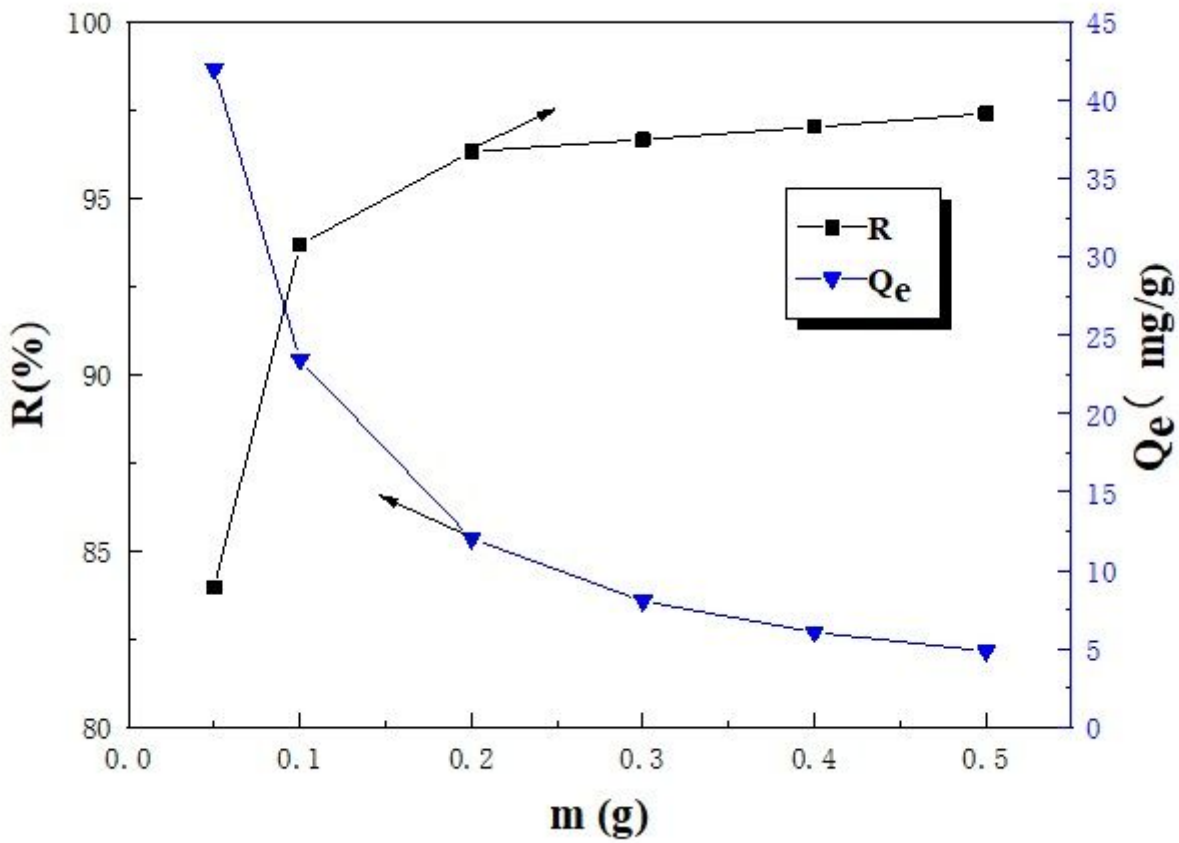


Figure 10

Effect of initial concentration of AR 73 solution on adsorption properties

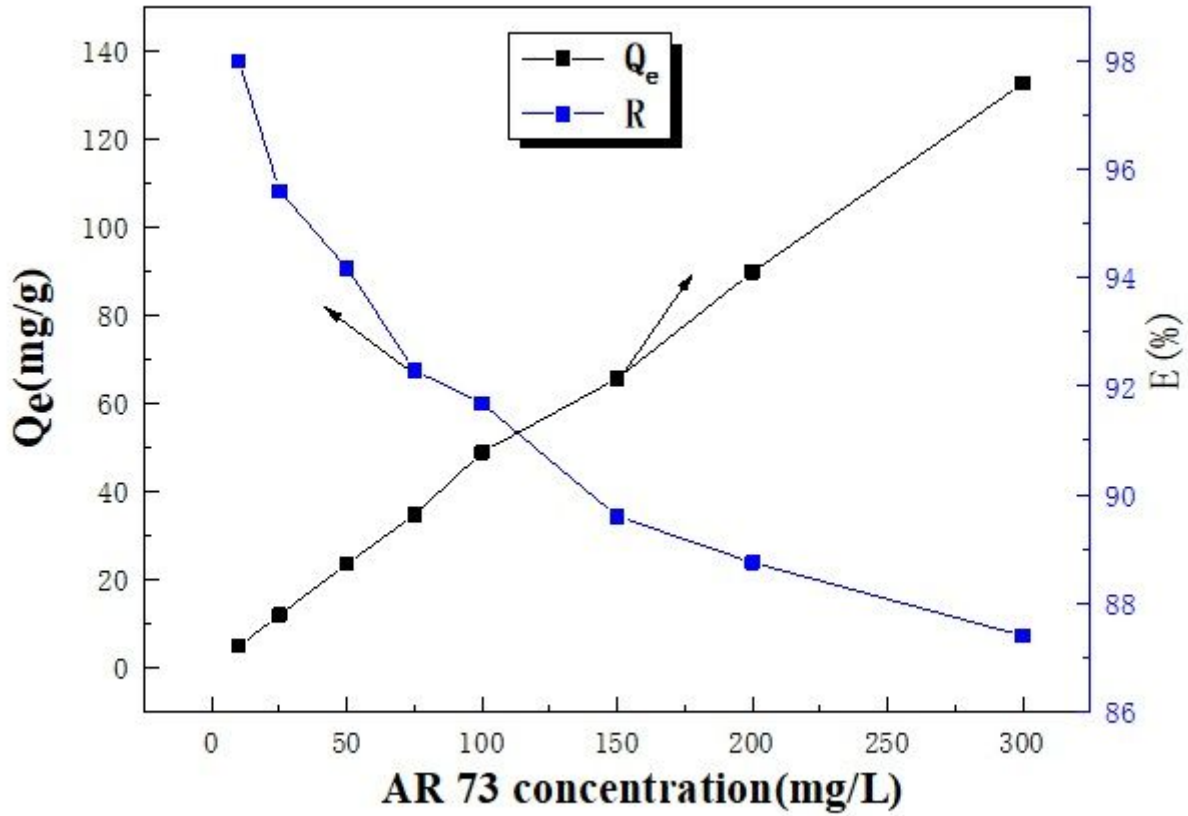


Figure 11

Effect of initial concentration of AR 73 solution on adsorption properties

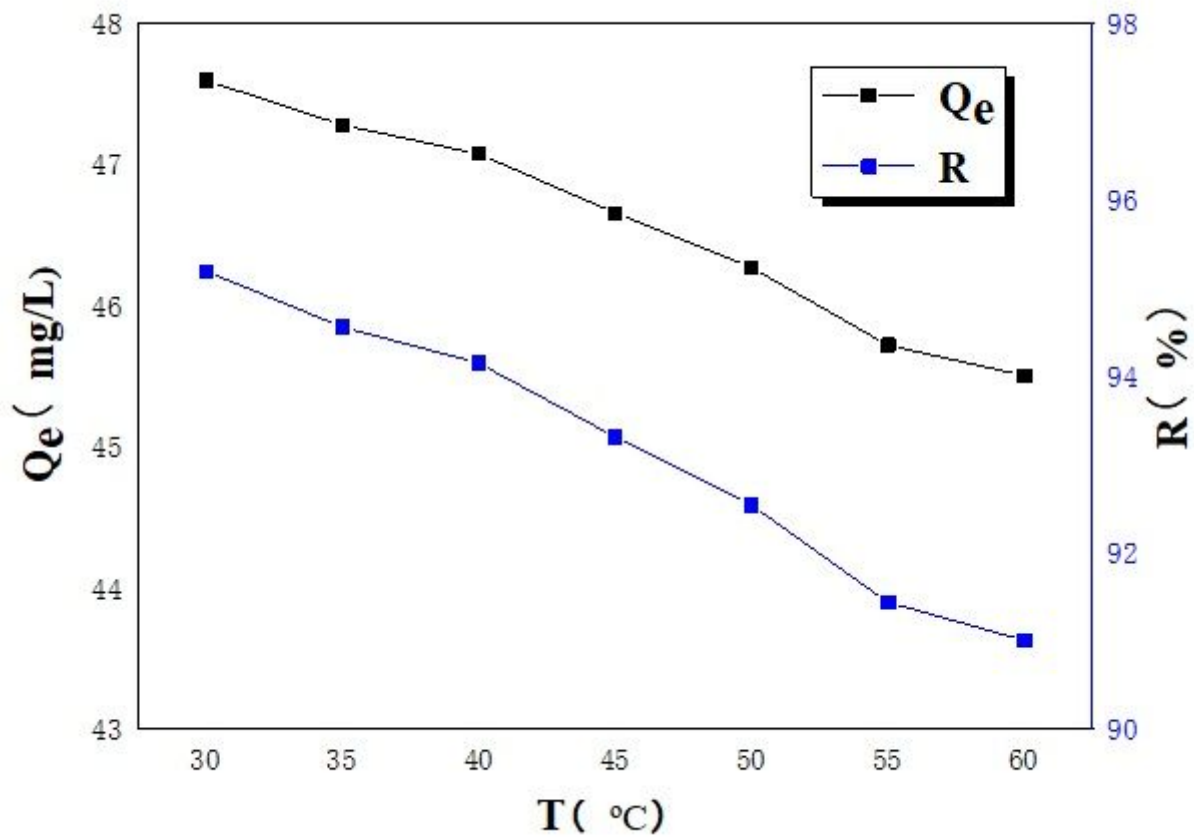
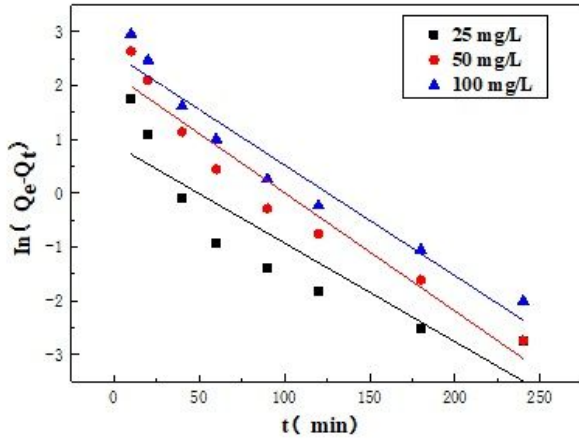


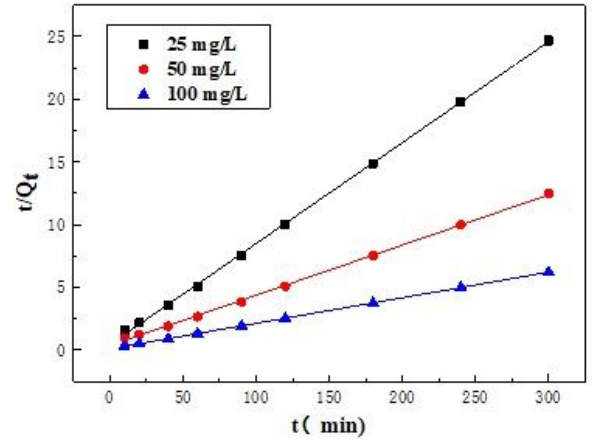
Figure 12

Effect of temperature on adsorption properties

(a)



(b)



(c)

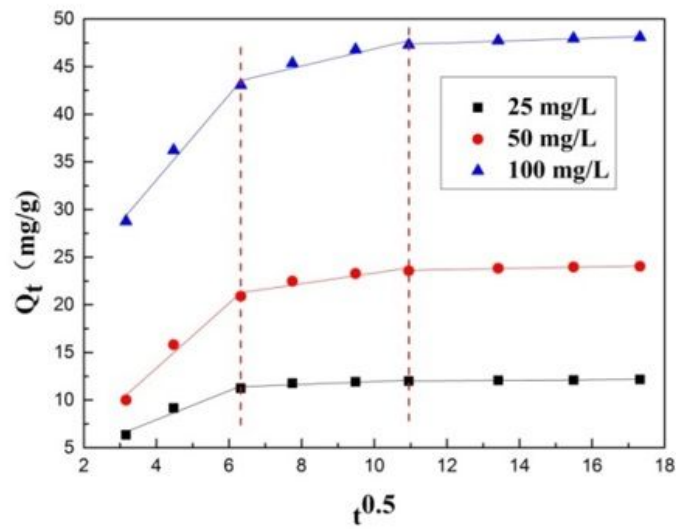


Figure 13

Kinetic models of acid red 73 at different concentrations:(a) pseudo-first-order kinetic model,(b) pseudo-second-order kinetic model,(c) Internal diffusion model

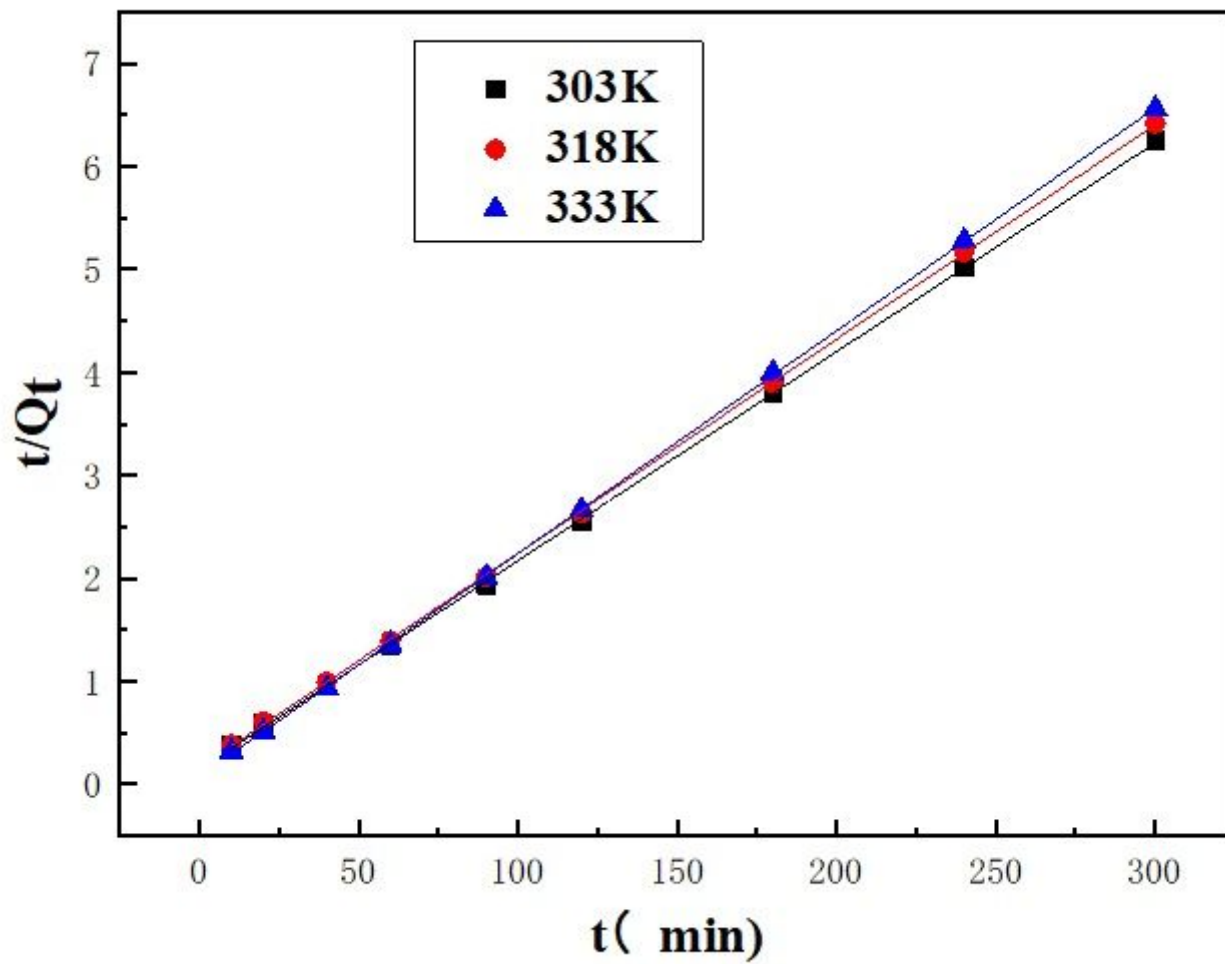
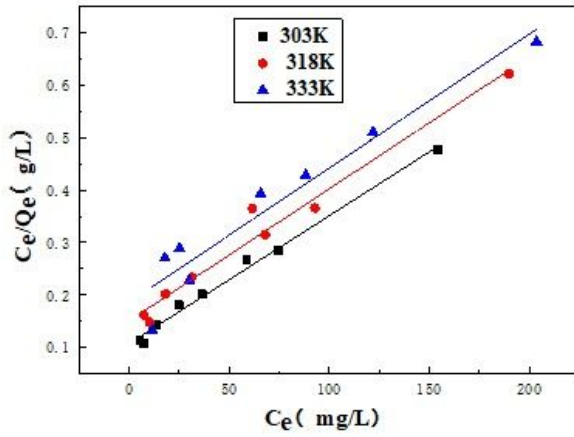


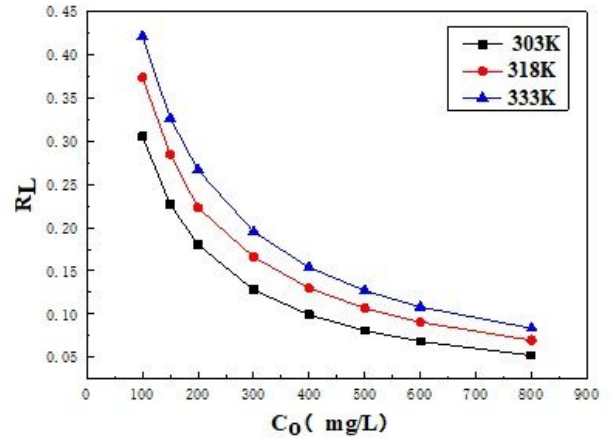
Figure 14

Pseudo-second-order kinetic model of AR 73 at different temperatures

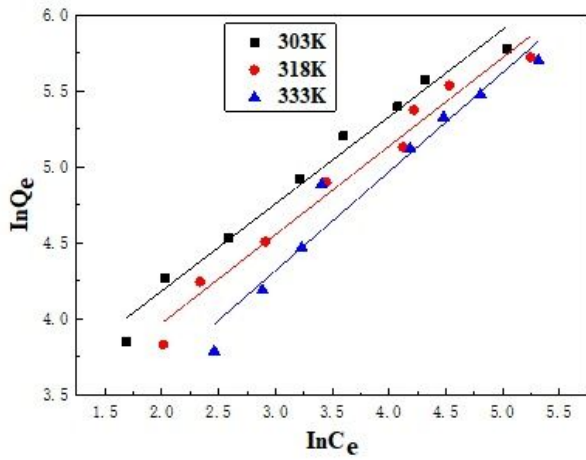
(a)



(b)



(c)



(d)

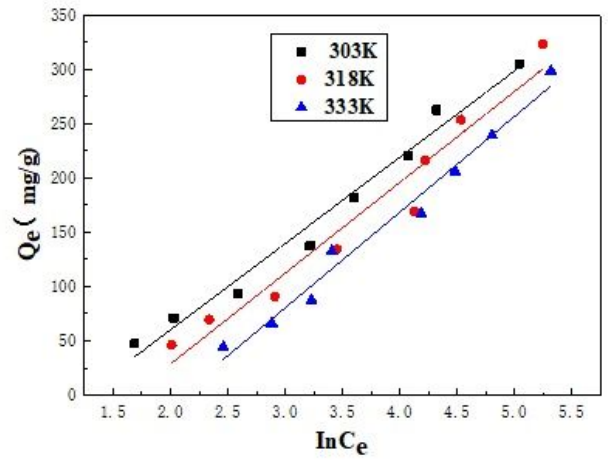


Figure 15

Adsorption isotherms at different temperatures (a) Langmuir (b) Relationship between  $RL$  and  $C_0$  at different temperatures (c) Freundlich (d) Temkin

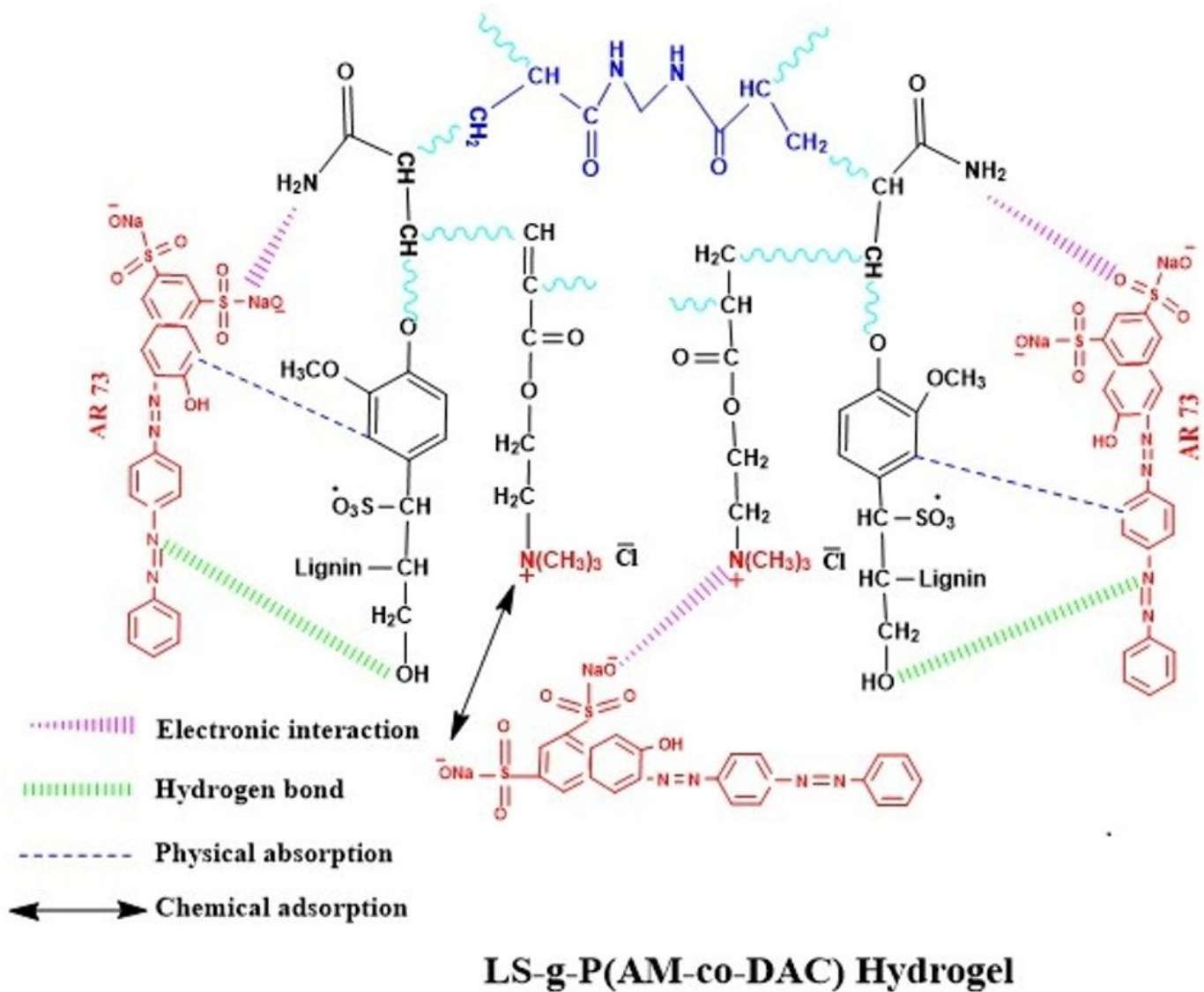


Figure 16

The adsorption mechanism of LAD hydrogel adsorbent